Received: 5 June 2024 | Revised: 31 March 2025 | Accepted: 3 April 2025

DOI: 10.1111/ppl.70249

ORIGINAL RESEARCH

Physiologia Plantarum

Do guard cells have single or multiple defense mechanisms in response to flg22?

Zalán Czékus[1] | András Kukri[1,2] | Atina Martics[1,2] | Boglárka Pollák[1] | Árpád Molnár[1] | Attila Ördög[1] | Györgyi Váradi[3] | László Galgóczy[4] | Rebeka Papp[2,4] | Liliána Tóth[4] | Katalin Ágnes Kocsis[5] | Nóra Faragó[6] | Nikolett Bódi[5] | Mária Bagyánszki[5] | Gabriella Szalai[7] | Kamirán Áron Hamow[7] | Péter Poór[1]

[1]Department of Plant Biology, Institute of Biology, Faculty of Science and Informatics, University of Szeged, Szeged, Hungary

[2]Doctoral School of Biology, University of Szeged, Szeged, Hungary

[3]Department of Medical Chemistry, University of Szeged, Szeged, Hungary

[4]Department of Biotechnology, Institute of Biology, Faculty of Science and Informatics, University of Szeged, Szeged, Hungary

[5]Department of Physiology, Anatomy and Neuroscience, Institute of Biology, Faculty of Science and Informatics, University of Szeged, Szeged, Hungary

[6]Avidin Ltd, Szeged, Hungary

[7]HUN-REN Centre for Agricultural Research, Martonvásár, Hungary

Correspondence
Péter Poór,
Email: poorpeti@bio.u-szeged.hu

Funding information
Emberi Erőforrások Minisztériuma, Grant/Award Numbers: ÚNKP-22-4, ÚNKP-22-5; Szegedi Tudományegyetem, Grant/Award Number: Open Access Fund (7050); Nemzeti Kutatási, Fejlesztési és Innovációs Alap, Grant/Award Numbers: FK 124871, FK 138867, PD146980

Edited by R.M. Rivero

Abstract

Bacterial flagellin (flg22) induces rapid and permanent stomatal closure. However, its local and systemic as well as tissue- and cell-specific effects are less understood. Our results show that flg22 induced local and systemic stomatal closure in intact tomato plants, which was regulated by reactive oxygen- and nitrogen species, and also affected the photosynthetic activity of guard cells but not of mesophyll cells. Interestingly, rapid and extensive local expression of *Ethylene response factor 1* was observed after exposure to flg22, whereas the relative transcript levels of *Defensin* increased only after six hours, especially in systemic leaves. Following local and systemic ethylene emission already after one and six hours, jasmonic acid levels increased in the local leaves after six hours of flg22 treatment. Using immunohistochemical methods, significant defensin accumulation was found in the epidermis and stomata of flg22-treated leaves and above them. Immunogold labelling revealed significant levels of defensins in the cell wall of the mesophyll parenchyma and guard cells. Furthermore, single cell qRT-PCR confirmed that guard cells are able to synthesise defensins. It can be concluded that guard cells are not only involved in the first line of plant defense by regulating stomatal pore size, but can also defend themselves and the plant by producing and accumulating antimicrobial defensins where phytopathogens can penetrate.

1 | INTRODUCTION

During their life, plants are exposed to various stresses, which can be abiotic and biotic (Nawaz et al., 2023). Among biotic stressors, phytopathogens can be classified as biotrophs, hemibiotrophs and necrotrophs based on their modes of plant infection (Meisrimler et al., 2021). Together, these have led to the evolution of diverse sensing and signalling pathways in plants (Han, 2019), resulting in a complex 'immune system' to induce defense responses that inhibit the harmful effects of microbial attacks and control their metabolism (Ngou et al., 2022). Key components of this system are the transmembrane pattern recognition receptors (PRRs), which are cell-surface-localized receptor kinases (RKs) or receptor proteins (RPs) sensing various phytopathogens by detecting microbial- (MAMPs) or pathogen-associated molecular patterns (PAMPs). This step triggers the first layer of plant defense responses, the PAMP-triggered immunity (PTI; DeFalco and Zipfel, 2021). At the same time, pathogens have developed various effector proteins and toxins to suppress PTI which are detected by intracellular nucleotide-binding leucine-rich repeat receptors (NLRs; Duxbury et al., 2021). Therefore, these effectors can also activate the effector-triggered immunity (ETI) in plants as the second layer of the defense reactions including a localized cell death killing the invading pathogens and preventing their spread within the plant tissues, termed as hypersensitive response (HR). In addition, systemic responses in their distal organs triggered by the infected ones can also be activated in a short time (within 6 hours), promoting a resistance to secondary pathogen infections, known as systemic acquired resistance (SAR; Johns et al., 2021; Vlot et al., 2021). Key components of PTI are the activation of Ca^{2+}-mediated signalling, rapid production of reactive oxygen- (ROS) and nitrogen (RNS) species, the activation of mitogen-activated protein kinases (MAPKs), the rapid local and systemic stomatal closure, the activation of defense-related hormone signalling, transcriptional reprogramming, accumulation of antimicrobial peptides such as defensins and callose deposition in the cell wall (DeFalco and Zipfel, 2021; Vlot et al., 2021; Myers et al., 2024).

Cell surface PRRs play a role in the sensing of MAMPs such as flg22, a 22 amino acid-long peptide from a conserved region of the N-terminus of the bacterial flagellin or chitosan, a deacetylated derivative of the fungal cell wall-composing chitin (Czékus et al., 2021a; Sanguankiattichai et al., 2022). Flg22 is perceived by the Flagellin sensing 2 (FLS2)- Brassinosteroid insensitive 1-associated kinase 1 (BAK1) PRR immune complex which phosphorylates the Botrytis-induced kinase 1 (BIK1) and then activates the plasma membrane-localized NADPH oxidase AtRBOHD in Arabidopsis (Lee et al., 2020). In tomato plants, the FLS2 receptor also perceives the major bacterial MAMPs such as flgII-28 and $flg15^{E\ coli}$ (Roberts et al., 2020). In addition, the FLS3 receptor has been also described in the tomato plant which also recognizes the epitopes of flagellin, such as flgII-28 (Sobol et al., 2023). Following the recognition of bacterial flagellin, rapid ROS production was measured in plant cells (Wu et al., 2023). ROS are generated by NADPH oxidase which can activate the plasma membrane-localized Ca^{2+} channels in stomata within minutes (Mittler et al., 2022) and subsequently the SLAC1 anion channel as well as aquaporin PIP2;1, which result in rapid stomatal closure (Liu et al., 2022). In addition to RBOHD, mitogen-activated protein kinases (MPKs), such as MPK3 and MPK6 are also activated and contribute to rapid stomatal closure upon flagellin perception (Wang et al., 2018; Zou et al., 2021).

Rapid stomatal closure upon detection of MAMPs is one of the earliest plant responses to phytopathogen attacks, preventing further penetration (Melotto et al., 2024). Stomatal closure is promoted by ROS and RNS and is regulated by the environment such as light, circadian rhythm, temperature, or humidity (Driesen et al., 2020; Czékus et al., 2021b). At the same time, the duration of stomatal closure depends on the ROS/RNS levels, which are regulated by defense-related phytohormones, such as salicylic acid (SA), jasmonic acid (JA), ethylene (ET), and abscisic acid (ABA; Wang et al., 2020; Myers et al., 2023). Based on previous observations, flg22 treatment inhibited the light-induced stomatal opening in the epidermal peels of Arabidopsis (Zhang et al., 2008) or it closed the stomata in intact leaves of Arabidopsis within 50 min (Deger et al., 2015). Interestingly, it was demonstrated that ABA biosynthesis is not required for flg22-induced stomatal closure (Payá et al., 2024), but the positive effects of ET (Mersmann et al., 2010; Czékus et al., 2021b) and JA (Hillmer et al., 2017) have also been reported in this process. Furthermore, the role of these hormones was also confirmed not only in the local responses to flg22, but also in the systemic defense responses of intact tomato plants (Czékus et al., 2021b). Furthermore, flg22 induced the local expression of the plant *defensin 1.2* gene (*PDF1.2*) within 4 h (Aslam et al., 2009) and callose deposition already after 6 hours in Arabidopsis leaves (Po-Wen et al., 2013) as a part of long-term defense responses. In addition to plant defensins, activation of the biosynthesis of other antimicrobial compounds, such as phytoalexin and camalexin has also been described in roots within 3 h (Millet et al., 2010). At the same time, these changes in the leaves are highly regulated by defense-related phytohormones such as JA and ET (Zhou et al., 2022). It has been well described that flg22 induces time-dependent and phytohormone-regulated changes in gene expression patterns throughout the leaf (Hillmer et al., 2017), but these changes at the single cell level, particularly in guard cells locally and systemically, have not been explored yet.

In this work, the defense responses induced by flg22 in mesophyll and guard cells were studied and compared with those in intact tomato plants. The main aim of this research was to find out whether the cells involved in the first line of defense in plants are able to defend themselves. We also investigated how and which defense signals are activated in these cells upon exposure to flg22, and whether these changes are cell-specific, local or systemic.

2 | MATERIALS AND METHODS

2.1 | Plant growing and experimental conditions

Intact tomato plants (*Solanum lycopersicum* L. cv. Ailsa Craig) were used for the experiments. The seeds were re-hydrated by soaking

them in water for 2 h, then germinated on wet filter paper in a thermostat for three days at 27°C. Then, healthy seedlings were placed in perlite and irrigated with water in a greenhouse under controlled environmental conditions (200 µmol m^{-2} s^{-1} photosynthetic flux density with LED lights, (PPFD; white LED (5700 K) supplemented with FAR LEDs; PSI, Drasov) a 12/12 h light/dark period (6:00–18:00 light period; 18:00–6:00 dark period), 24/22°C day/night temperatures and 55%–60% relative humidity (Czékus et al., 2021b). After two weeks of incubation, the plants were transferred to 500 mL pots containing tomato nutrient solution (2 mM $Ca(NO_3)_2$, 1 mM $MgSO_4$, 0.5 mM KH_2PO_4, 0.5 mM Na_2HPO_4, 0.5 mM KCl, 0.02 mM Fe(III)-EDTA and micronutrients (0.001 mM $MnSO_4$, 0.005 mM $ZnSO_4$, 0.0001 mM $CuSO_4$, 0.0001 mM $(NH_4)_6Mo_7O_{24}$, 0.0001 mM $AlCl_3$, 0.0001 mM CoCl, 0.01 mM H_3BO_3; pH 5.8) according to Poór et al., (2019). The nutrient solution was changed three times a week.

2.2 | Flagellin22 treatments

The abaxial side of tomato leaves from the sixth leaf node of intact plants was treated with 5 µM flg22 (Genscript Biotech Corporation) by applying it using a squirrel hairbrush in the morning (8:00 a.m.) without wounding or disturbing the leaves (Korneli et al., 2014; Czékus et al., 2023). Local and systemic defense responses of the plants were assessed 1 and 6 h later in the leaves from the sixth node from the shoot apex (treated, flg22) and from the distal fifth node (not treated, flg22 + 1) above the flg22-treated leaves. Sterile distilled water without flg22 was used for untreated controls.

2.3 | Measurement of stomatal aperture size

Abaxial epidermal strips were rapidly prepared from the selected leaves of the plants and immediately examined under a microscope (Nikon Eclipse TS-100, Nikon Instruments) according to the method of Melotto et al., (2006). Stomatal aperture width was determined using the Image-Pro Plus 5.1 software (Media Cybernetics, Inc.,). For each treatment, leaves from three different plants were used for sampling. Stomata (90–120) from three different plants were recorded.

2.4 | Determination of stomatal conductance

Stomatal conductance (gs) was determined in the middle of the central part of tomato leaves using a steady-state porometer (PMR-2, PP Systems) under greenhouse conditions (Gallé et al., 2013).

2.5 | Determination of photosynthetic activity in guard and mesophyll cells

Chlorophyll fluorescence of guard and mesophyll cells was examined using a microscopy-PAM chlorophyll fluorometer (Heinz Walz) mounted on a Zeiss Axiovert 40 inverted epifluorescence microscope (Carl Zeiss Inc.) with a PAM-2000 (Heinz Walz) according to the method of Goh et al., (1999) and Poór and Tari (2012). To determine the photosynthetic activity in guard cells, abaxial epidermal strips were rapidly prepared from the treated and distal leaves of intact plants. Then the strips were immediately transferred to glass-bottom culture dishes (MatTek Co.) containing 3.5 mL of buffer solution (10 mM 2-(N-morpholino) ethanesulfonic acid (MES), 10 mM KCl, pH 6.15) based on Zhang et al., (2001). Before measuring the minimal fluorescence yield of the dark-adapted state (F_0), the samples were kept in dark for 15 min. Firstly, the maximal fluorescence in the dark-adapted state (F_m) was determined after the dark adaption. During the experiments, the following parameters were calculated: the maximal quantum efficiency of PSII photochemistry [$F_v/F_m = (F_m - F_0)/F_m$], the actual quantum yield of PSII electron transport in the light-adapted state [$\Phi PSII = (F_m' - F_s)/F_m'$], the photochemical quenching coefficient [$qP = (F_m' - F_s)/(F_m' - F_0')$], and the light-induced photoprotection through thermal dissipation of energy as [$NPQ = (F_m - F_m')/F_m'$] using the formula of Genty et al., (1989) and Kramer et al., (2004), respectively. Three leaves from three different plants were measured in the case of all treatments.

2.6 | Detection of stomatal ROS and NO production

10 µM dihydroethidium (DHE; Sigma-Aldrich) and 50 µM 10-acetyl-3,7-dihydroxyphenoxazine (AR; ADHP or Ampliflu™ Red; Sigma-Aldrich) fluorescent dyes were used to detect stomatal superoxide and H_2O_2 production in accordance with the method of Poór et al., (2015). Subsequently, samples were incubated in the dark in the presence of specific dyes at room temperature for 30 min and then washed twice with 10 mM Tris(hydroxymethyl)aminomethane (TRIS–HCl, pH 7.4) buffer. For stomatal NO detection, 10 µM 4-amino-5-methylamino-2′,7′-difluorofluorescein diacetate (DAF-FM DA; Sigma-Aldrich) prepared in 10 mM 10 mM 2-(N-morpholino) ethanesulfonic acid (MES)/ potassium chloride (KCl) buffer (pH 6.15) was used according to the protocol of Bright et al., (2006) in the same way as for ROS detection. After the incubation, the samples were washed two times for 10 min with MES/KCl buffer (pH 6.15). The fluorescence intensity of the samples after staining was detected using a Zeiss Axiowert 200 M type fluorescence microscope (Carl Zeiss Inc.) and measured using the AxioVision Rel. 4.8 software (Carl Zeiss Inc.) after taking digital photos with a high-resolution digital camera (Axiocam HR, HQ CCD camera) with the filter set 10 (excitation 450–490 nm, emission: 515–565 nm), the filter set 20HE (excitation: 535–585 nm, emission: 600–655 nm) and the filter set 9 (excitation: 450–490 nm; emission: 515–∞ nm; Czékus et al., 2022). Fluorescence intensities (pixel intensity) were measured on digital images within the areas of stomata using the Axiovision Rel. 4.8 software (Carl Zeiss Inc.). Stomata (30–40) from four leaves of different plants were measured for all treatments.

2.7 | Measurements of ROS and NO levels in the leaves

For the determination of superoxide production in leaves, 100 mg of tissue was homogenized in 1 mL of ice-cold sodium phosphate buffer (100 mM, pH 7.2) containing 1 mM sodium diethyldithiocarbamate trihydrate (Sigma-Aldrich), then centrifuged (13 000 *g* for 15 min at 4°C) and 300 µL of the supernatant was added to the reaction mixture containing 650 µL of 100 mM sodium phosphate buffer (pH 7.2) and 50 µL of 12 mM nitro blue tetrazolium. Absorbance was measured before (A0) and after 5 min incubation (AS) at 540 nm using a spectrophotometer (KONTRON). Superoxide production was calculated using the formula ΔA540 = AS - A0 and expressed as ΔA540 (min^{-1} g^{-1} fresh weight; Kukri et al., 2024).

For the determination of the H_2O_2 level, 200 mg of leaf tissue was homogenized with 1 mL of ice-cold 0.1% trichloroacetic acid (TCA) and after centrifugation (11 500 *g* for 10 min at 4°C), 250 µL of the supernatant was added to a reaction mixture containing 250 µL of 50 mM potassium phosphate buffer (pH 7.0) and 500 µL of 1 M potassium iodide (KI). After 10 min of incubation at room temperature, the absorbance was measured at 390 nm using a spectrophotometer (KONTRON; Ashraf et al., 2022). The H_2O_2 content was determined using a standard curve constructed from a standard series containing 0, 1, 2, 3, 4, 5, 6, 7, 8, 9, and 10 µM H_2O_2 (Sigma-Aldrich).

NO production was determined in leaf discs from control and flg22-treated leaves of intact plants as well as in upper leaves infiltrated with 10 µM DAF-FM DA dissolved in 10 mM Tris–HCl buffer (pH 7.4) under vacuum for 30 min in the dark at room temperature. After incubation, the samples were rinsed twice in 10 mM Tris–HCl buffer (pH 7.4). The fluorescence intensity was detected using a Zeiss Axiowert 200 M fluorescence microscope (Carl Zeiss Inc.) equipped with a high-resolution digital camera (Axiocam HR, Carl Zeiss Inc.) and determined at 515–565 nm with an excitation at 450–495 nm. The data were analyzed using the AXIOVISION REL. 4.8 software (Carl Zeiss Inc.,) according to Poór et al., (2015).

2.8 | Determination of ethylene and jasmonic acid content in leaves

Ethylene production from control, treated, and systemic leaves of intact plants was measured using a Hewlett-Packard 5890 Series II gas chromatograph (GC) equipped with a flame ionization detector and an activated alumina-packed column, according to the method of Poór et al. (2015). The sample (0.5 g) was collected in gas-tight flasks (10 mL) and incubated for 1 h in the dark. The flasks contained 0.5 mL of deionized water to avoid dehydration of the samples. After the incubation period, 2.5 mL of gas was removed from the flasks and injected into the GC using a gas-tight syringe (Hamilton Co.). The flow rate of helium carrier gas was 35 cm^3 min^{-1}, that of hydrogen was 30 cm^3 min^{-1} and in case of air was 350 cm^3 min^{-1}. The temperature of the injector was 120°C, that of the column was 100°C and in case of the flame ionization detector was 160°C. The concentration of ethylene was determined by preparing a tenfold dilution series in gas-tight flasks with a gas-tight syringe, using an ethylene standard (Messer Hungarogas Ltd.). Leaves from six different plants were used for all measurements and the experiment was repeated three times with a new generation of plants ($n = 3$). Means ± SE were calculated based on all data from the three biological replicates.

The jasmonic acid content was determined according to Pál et al., (2019). Portions of 0.2 g of liquid N_2 homogenized plant leaves were transferred into 2-ml safety Eppendorf tubes. Prior to extraction, the samples were spiked with 20 ng of [$^2H_6$] (+)-*cis,trans*-abscisic acid (OlChemIm s.r.o.) as an internal standard. Extraction was performed using a volume of 1 mL of a methanol:water (2:1) mixture, followed by 5 sec of vigorous vortexing. The samples were then subjected to shaking with a Spex Mini G 1600 in a cryo-cooled rack for 3 min. Following centrifugation (16 500 *g*, 10 min, 4°C), the extracts were collected, and the remaining pellets were subjected to a second extraction cycle. The methanol–water sample solution was then subjected to liquid–liquid partitioning by the addition of 1 mL of n-hexane (VWR), in order to remove apolar matrix components. Subsequently, centrifugation (10 000 *g*, 10 min, 4°C) was performed to collect the lower methanol–water phase, which was then filtered through a 0.22 µm PTFE syringe filter. The filtrate was transferred to borosilicate vials and analyzed with 2 µL of samples injected. The separation process was accomplished on a Waters HSS T3 column (1.8 µm, 100 mm × 2.1 mm) utilising an Acquity I class UPLC system (Waters Corp.). The separation was achieved through gradient elution with 0.1% (v/v) formic acid, both in water (A) and acetonitrile (B). Tandem mass spectrometry detection was performed in multiple reaction monitoring (MRM) mode on a Xevo TQ-XS (Waters) equipped with a UniSpray™ source. Reference materials employed for identification and quantitation were purchased from the Merck-Sigma Group.

2.9 | Gene expression analysis in the leaves

To extract total RNA from leaf samples, 1 mL of TRI reagent (1.82 M guanidium isothiocyanate, 11.36 mM sodium citrate, 200 mM potassium acetate (pH 4.0), 0.73 mM N-laurylsarcosine, 45.45% phenol) was added to approximately 100 mg of leaf sample previously homogenized in liquid nitrogen to a fine powder (Takács et al., 2018). Following that, the samples were incubated at 65°C for 3 min and 200 µL of chloroform was added to the samples. After centrifugation (11 180 *g*, 15 min, 4°C), the supernatant was added into 375 µL of chloroform:isoamyl alcohol (24:1) and centrifuged again (11 180 *g*, 15 min, 4°C). The supernatant was added into 500 µL of isopropanol and incubated for 10 min at room temperature. After centrifugation, the pellet was cleaned with 500 µL of 70% ethanol, then dissolved in 30 µL of of molecular biology water (AccuGENE®, Lonza Group Ltd.). Genomic DNA was digested with DNase I (Thermo Fisher Scientific). The RNA content of the samples was measured using a NanoDrop™ 1000 spectrophotometer (NanoDrop Technologies). The cDNA was synthesised using MMLV reverse transcriptase (Thermo Fisher Scientific) and random hexamer

primers (Thermo Fisher Scientific). The selected tomato genes (*SlERF1* (Solyc05g051200); *SlDEF* (Solyc07g007760)) were obtained from the Sol Genomics Network (SGN; http://solgenomics.net/) database and the relative transcript levels were analyzed by quantitative real-time reverse transcription-PCR (qRT-PCR; qTOWER Real-Time qPCR System, Analytik Jena). The PCR mixture contained 5 µL of Maxima SYBR Green qPCR Master Mix (2X; Thermo Fisher Scientific), 3 µL of Molecular Biology Water (AccuGENE®, Lonza Group Ltd), 400–400 nM forward and reverse primers and 10 ng cDNA template in a final volume of 10 µL. After an initial denaturation step (95°C, 7 min), the qPCR programme consisted of 40 cycles of denaturation (95°C, 15 s) and annealing extension (60°C, 60; Takács et al., 2018). The data were analyzed using the $2^{(-\Delta\Delta Ct)}$ formula (Livak and Schmittgen, 2001) with reference housekeeping genes (qTOWER Software 2.2; Analytik Jena). As references, elongation factor-1α subunit (*SlEF1α* (Solyc06g005060)) and 18S ribosomal RNA (*Sl18S* (GQ280796)) were used. Data were normalized to the transcript levels of the reference genes and to the transcript levels of untreated control leaves. For each sample, leaves from at least three different plants were collected, mixed and used.

2.10 | Immunofluorescence detection of defensins

The peptide fragment, according to the consensus sequence of tomato plant defensins, was designed (Ac-GFSGGNC(-SH)RGFRRRC (-SH)F-NH_2) and used as antigens for the production of polyclonal antibodies in rabbits (Davids Biotechnologie GmbH). The sera were antigen affinity purified and used for immunofluorescence detection of defensins. For the immunofluorescence detection of defensins, epidermal peels were prepared and placed in TBSA-BSAT buffer (5 mM Tris, 0.9% NaCl, 0.05% sodium azide, 0.1% BSA and 0.1% Triton X-100; pH 7.2) containing anti-DEF (1:2500; Davids Biotechnologie GmbH) for 1 h at room temperature in the dark. The samples were then washed quickly three times with TBSA-BSAT and then labelled with the secondary FITC-conjugated rabbit antibody (Agrisera AB) for 1 h. The samples were then washed quickly three times with TBSA-BSAT. For microscopic analysis, the samples were transferred to slides into PBS:glycerol (1:1) and the green fluorescence of the samples was detected using a Zeiss Axiowert 200 M fluorescence microscope (Carl Zeiss Inc) equipped with a high-resolution digital camera (Axiocam HR, Carl Zeiss Inc.). Data were analysed using the AXIOVISION REL. 4.8 software (Carl Zeiss Inc.) according to Kolbert et al., (2023). Leaves from three different plants were used for all measurements.

2.11 | Post-embedding immunohistochemistry and transmission electron microscopy

For post-embedding electron microscopy, leaf segments (5–6 mm) were fixed in 2% (w/v) paraformaldehyde and 2% (w/v) glutaraldehyde solution immediately after the 6 h samplings and then further fixed for 1 h in 1% (w/v) OsO_4. After rinsing in 0.1 M phosphate buffered saline (PBS, pH 7.4) buffer and dehydrating in increasing concentrations of ethanol (50%, 70%, 96%, 100%) and acetone, leaf segments were embedded in Embed812 (Electron Microscopy Sciences). Semi-thin (0.7 µm) sections were cut from the embedded blocks to select the area of interest, and ultrathin (70 nm) sections were mounted on nickel grids. To investigate the effects of flg22 treatments on the quantitative changes in defensin, three grids of ultrathin sections from each block were processed for immunogold labelling (Poór et al., 2019). Briefly, the grids were incubated overnight with rabbit polyclonal anti-DEF primary antibody (Davids Biotechnologie GmbH; final dilution 1:100) followed by protein A-gold-conjugated anti-rabbit secondary antibody (18 nm gold particles, Jackson Immuno Research; final dilution 1:20) for 3 h with extensive washing with 0.2 M Tris-buffered saline (TBS, pH 7.4) buffer between steps. The specificity of the immunoreaction was assessed in all cases by omitting the primary antibody from the labeling protocol and incubating the sections in the protein A-gold-conjugated secondary antibody alone (Sup Figure 1). The sections were counterstained with uranyl acetate (Merck) and lead citrate (Merck) and then examined and photographed using a JEOL JEM 1400 transmission electron microscope (TEM; Jeol Ltd.). The number of gold particles, assumed to label defensin, was determined in the wall of 4–6 guard cells, three epidermal cells and three mesophyll cells per experimental group. Counting was performed on digital photographs at 15 000× magnification using the AnalySIS 3.2 program (Soft Imaging System GmbH). Data were expressed as the total number of gold particles per unit area of the cell types analyzed. Leaves from three different plants were used for the measurements.

2.12 | Sampling and analysis of single-cell qRT-PCR

Leaves from flg22-treated, above them (flg22 + 1), control as well as control+1 leaf levels were peeled, then 60 individual stomata were extracted immediately from the epidermal cell layer by laser microdissection (Zeiss PALM MicroBeam System). Samples were collected in PCR tube caps containing 3 µL 10× SingleCellProtect™ (Avidin Ltd.) buffer according to the method of Brasko et al., (2018). Three leaves from three different plants were peeled in the case of all treatments which were repeated independently three times with a new generation of plants ($n = 3$). After collection, all tubes were closed and immediately stored at -80°C.

Samples were first incubated for 5 min at 65°C in a mixture of 3 µL 1× SingleCellProtectTM (Avidin Ltd), 0.3 µL primer mix, 0.3 µL 10 mM dNTPs (Thermo Fisher Scientific), 1 µL 5× first strand buffer, 0.3 µL 0.1 mol/L DTT, 0.1 µL RNase inhibitor (Thermo Fisher Scientific) and 100 U reverse transcriptase (Superscript III, Thermo Fisher Scientific). The reaction was then performed at 55°C for 1 h and stopped by heating at 75°C for 15 min. The reverse transcription reaction mixture was stored at −20°C.

The single-cell qRT-PCR was performed on a LightCycler® Nano RT-PCR instrument (Roche) in a total volume of 20 µL containing 5 µL cDNA, 1 µL forward and reverse primer pairs of *SlDEF* (Solyc07g007760) and 10 µL qPCRBIO Master Mix Lo-ROX

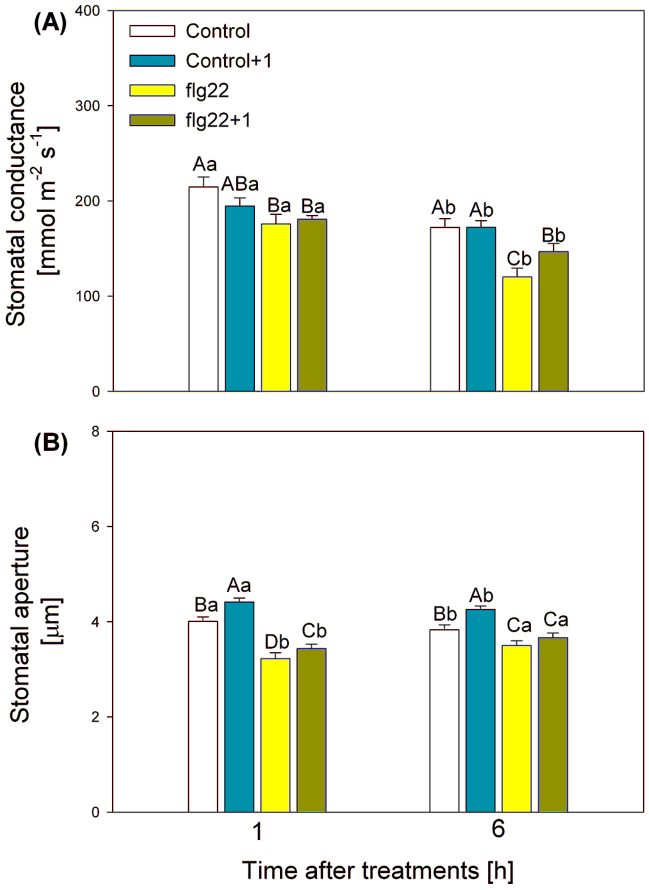

FIGURE 1 Time-dependent regulation of stomatal activity. Changes in the stomatal conductance (A) and the size of stomatal apertures (B) were examined in the abaxial epidermal strips of intact tomato plants treated foliar with 5 µM flagellin (flg22) at 8:00 a.m. Measurements were carried out one and six hours after treatments (at 9:00 a.m. and 14:00 p.m.). Means ± SE, $n = 3$. Means were analyzed by two-way ANOVA, and significant differences among the data were analyzed by Duncan's test. Mean values significantly different at $p < 0.05$ were signed with different letters, upper case letters indicate the effects of the treatment at the same daytime, and lower case letters indicate the effects of the daytime under the same treatment. (Control: treatment with sterile distilled water; Control+1: untreated leaves from the distal node from the control; flg22: treatment with 5 µM flagellin dissolved in sterile distilled water; flg22 + 1: untreated leaves from the distal node from the flg22-treated one).

(Pcr Biosystems). The following cycling protocol was used: 5 min at 95°C followed by 50 cycles (10 secs at 95°C, 10 secs at 56°C and 15 min at 72°C). The LightCycler® Nano analysis software (Roche) determined a cycle threshold (CT) value, which identified the first cycle where fluorescence was detected above baseline.

2.13 | Statistical analysis

The experiments were repeated at least three times involving 9–9 plants per treatments. Results are expressed as mean ± SE. The effects of flg22 treatments locally and systemically and differences between time points were analyzed by two-way ANOVA, supplemented by post hoc pairwise comparisons using Duncan's multiple range test. All statistical analyses were performed using the SigmaPlot 11 software (Systat Software Inc.). Means marked with different letters are significantly different at $p < 0.05$.

3 | RESULTS

First, the direct and indirect effects of the bacterial elicitor flg22 on stomata were tested within six hours. Application of the bacterial elicitor flg22 at 08:00 a.m. induced rapid stomatal closure within 1 h locally and in the systemic leaves of intact tomato plants (Figure 1A, B), which persisted in the plants for 6 h (Figure 1A, B), based on the measurements of both stomatal conductance and stomatal aperture measurements. However, the stomata already started to close at 14:00 independently of treatments, which is essentially regulated by the circadian rhythm of the plants (Figure 1A, B).

As these are photosynthetic cells, the next step was to determine the changes in photosynthetic activity of guard cells of flg22-treated and systemic (flg22 + 1) leaves. Surprisingly, the photosynthetic activity of guard cells in leaves treated with flg22 was affected to a greater extent than that of the mesophyll cells (Figure 2). Although the maximum quantum yield parameter of PSII (F_v/F_m) did not change in guard cells of flg22-treated or systemic leaves (Figure 2A), the effective quantum yield of PSII (ΦPSII) and the photochemical quenching coefficient (qP) decreased significantly after 1 h in the guard cells of flg22-treated leaves as compared to the control, but did not change in the systemic (flg22 + 1) leaves (Figure 2C, E). In parallel, non-photochemical quenching (NPQ) increased significantly in these stomata after 1 and 6 h, both in the flg22-treated and systemic (flg22 + 1) leaves (Figure 2G). At the same time, no significant changes were observed in the mesophyll cells of flg22-treated and flg22 + 1 leaves, for all the parameters analyzed (Figure 2B, D, F, H).

In the next experiments, the signalling components of flg22-induced stress, such as ROS and NO production, were detected at the cellular and organ level in tomato plants. Treatment with flg22 resulted in significantly higher superoxide (Figure 3A), H_2O_2 (Figure 3B) and NO (Figure 3C) production in stomata already after 1 h. After 6 h, only superoxide production was significantly higher in stomata of flg22-treated leaves (Figure 3A), whereas significant superoxide (Figure 3A) and NO (Figure 3C) accumulation was measured in guard cells of systemic leaves (flg22 + 1) compared to their respective controls (Figure 3). Interestingly, H_2O_2 production did not change 6 h after flg22 exposure in stomata of elicitor-treated leaves (Figure 3B).

Changes in ROS and NO production were also determined in the leaves of tomato plants. Among the ROS, superoxide production was significantly induced after 1 h in flg22-treated leaves, but did not change in flg22 + 1 leaves (Figure 4A). After 6 h following treatments the superoxide production in the systemic control (control+1) as well as flg22 + 1 leaves was higher in respect to their relative controls, however no significant changes were found in the leaves from the

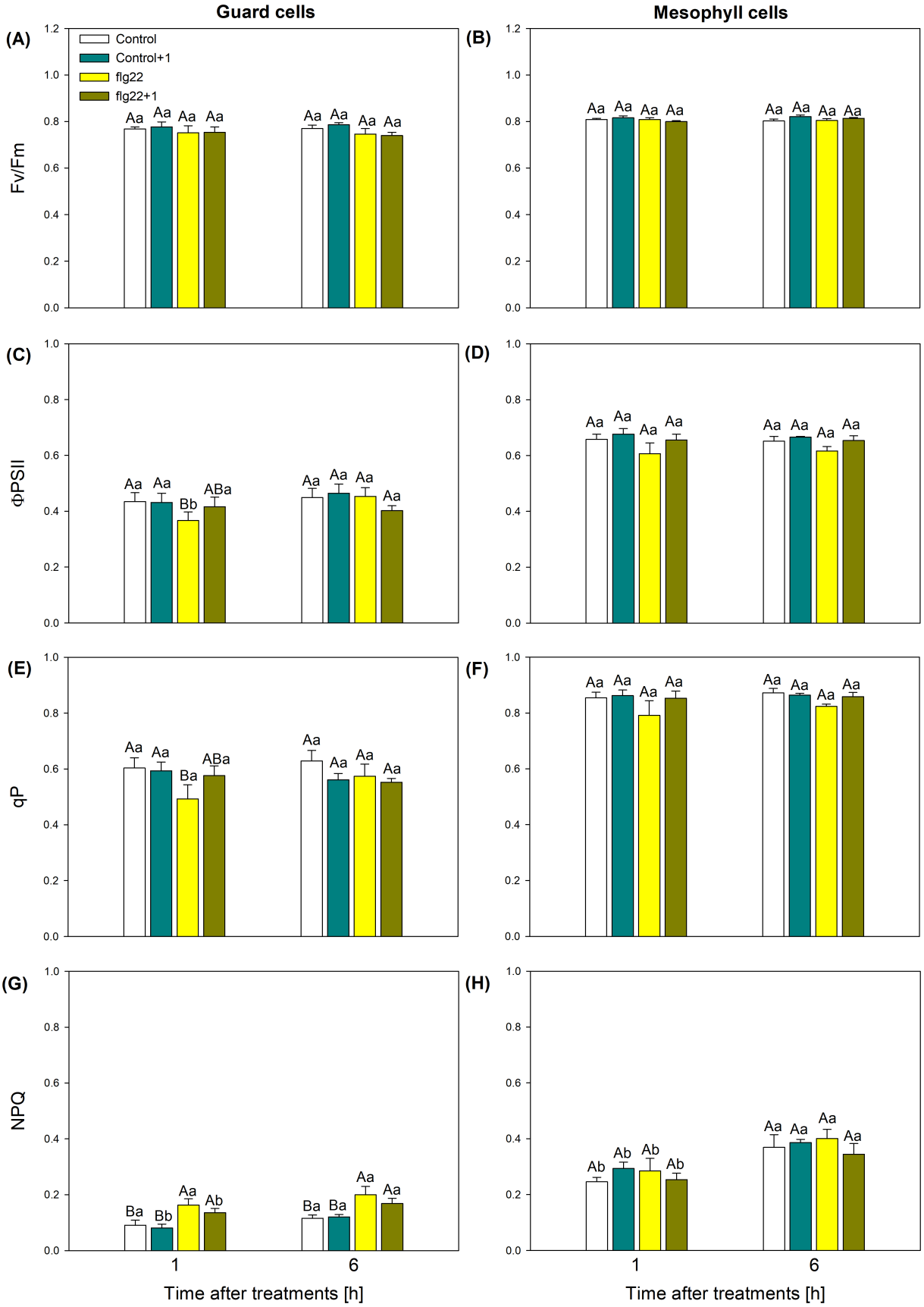

FIGURE 2 Legend on next page.

selected nodes 6 hrs later following flg22 treatments (Figure 4A). The H_2O_2 levels were slightly elevated in local and leaves after 1 h of flg22 treatments, but were significantly higher in systemic, flg22 + 1 leaves after 6 h (Figure 4B). At the same time, the NO productions of flg22-treated and flg22 + 1 leaves were significantly higher than that of controls after 1 h (Figure 4C). In addition, NO production was also significantly higher in the systemic flg22 + 1 leaves after 6 h (Figure 4C), similarly to the H_2O_2 content (Figure 4B).

Regarding flg22-induced defense signalling in plants, ET and JA levels were measured in tomato leaves 1 and 6 h after the bacterial elicitor treatments. While ET production was induced both locally and systemically immediately (1 h later) after flg22 exposure and was also significantly higher after 6 h (Figure 5A), JA levels increased only after 6 h, especially in the systemic leaves of the plants (Figure 5B).

Response marker genes of ET- and JA-induced signalling were also examined. The expression of the ET marker gene, *Ethylene response factor 1* (*SlERF1*) was basically higher in the systemic (control +1) leaves under control conditions. However it was further induced in the systemic leaves already after 1 h following flg22 treatment, while it was increased both locally and systemically 6 h later (Figure 6A). Interestingly, the tomato *Defensin* (*SlDEF*) was significantly up-regulated only 6 hours later in flg22-treated and untreated distal leaves of the intact plants (Figure 6B). At the same time, the expression of *SlDEF* was basically lower in the younger and upper leaves of the control plants.

DEF levels were further analysed at the protein level using epidermal peels from the flg22-treated tomato plants, at the time point (6 h later following flg22 treatments) when JA levels increased and significant expression of *SlDEF* was recorded. Based on the analysis of the fluorescence assay (Figure 7C), significant DEF accumulation was found in the epidermal cells (Figure 7A) and stomata (Figure 7B) of flg22-treated and flg22 + 1 systemic leaves of intact tomato plants after 6 h as compared to control.

Immunogold labeling and TEM were used to further analyze the localization of DEF in the different cell types of the leaves. Based on the results, significant DEF localization was observed in the cell walls of mesophyll-, epidermal- and guard cells (Figure 8). The highest amount of DEF-labelled gold particles was measured in the mesophyll cell wall (Figure 8A) compared to epidermal (Figure 8B) and guard cells (Figure 8C). The accumulation of DEF was basically higher in the cell wall of mesophyll cells of control+1 leaves as compared to local control leaves. At the same time, flg22 caused a significant accumulation of DEF, both locally and systemically in the cell wall of all the cell types that were examined (Figure 8), which was the highest in the case of flg22 in cell wall of stomata (69%), followed by the epidermis- (57%) and mesophyll cells (36%). Significant DEF accumulation was also observed in the cell wall of stomata after flg22 treatments, at the part where the two guard cells fit and close, respectively (Figure 8D).

To answer the question of whether guard cells are also capable of synthesising DEF, single cell qRT-PCR was used. The results showed that stomata themselves can induce the expression of *SlDEF*, which was also increased locally and systemically 6 hours after flg22 treatments (Figure 9). At the same time, the expression of *SlDEF* was basically lower in the stomata of younger and upper leaves of control plants, similar to that measured in the mesophyll cells (Figure 6B).

4 | DISCUSSION

The main objectives of this research were to study the local and systemic defense responses induced by flg22 at the cellular level in leaves of intact tomato plants, to identify the similarities and differences between the two cell types and to increase our knowledge about how guard cells, as part of the first line of plant defense, can defend themselves and the stressed plant.

It is well known that rapid stomatal closure is one of the first and key steps of plant defense responses to biotic (Panchal and Melotto, 2017; Melotto et al., 2024) and abiotic (Kollist et al., 2019; Matkowski and Daszkowska-Golec, 2023) stresses. However, the direct effects of stressors on guard cells and their own defense against stressors remained largely unclear. Furthermore, it has been described that flg22 induces rapid stomatal closure within minutes using in vitro stomatal assays (Montillet et al., 2013; Toum et al., 2016; Rodrigues et al., 2017) and in intact plants (Deger et al., 2015), but it is difficult to detect its long-term effects (Czékus et al., 2021b). Based on our previous results (Czékus et al., 2023) and the present experiments, it is suggested that flg22 induces not only local but also systemic stomatal closure in distal leaves of intact tomato plants (flg22 + 1; Figure 1). However, as the effect of flg22 on stomatal movement is dependent on the circadian rhythm, the closure induced by the bacterial elicitor was also detected 6 h later in the afternoon, both locally and systemically (Figure 1). Other researchers have also found that various stress-induced stomatal closure can be initiated locally and systemically as early as 10 minutes and

FIGURE 2 Time-dependent regulation of the photosynthetic activity of stomata and leaves of intact tomato plants. Changes in the maximum quantum yield of PSII (F_v/F_m), the effective quantum yield of PSII photochemistry (ΦPSII), the photochemical quenching coefficient (qP) and the non-photochemical quenching (NPQ) of stomata and leaves were examined in intact tomato plants treated foliar with 5 μM flagellin (flg22) at 8:00 a.m. Measurements were carried out one and six hours later after treatments (at 9:00 a.m. and 14:00 p.m.). Means ± SE, n = 3. Means were analyzed by two-way ANOVA, and significant differences among the data were analyzed by Duncan's test. Mean values significantly different at $p < 0.05$ were signed with different letters, upper case letters indicate the effects of the treatment at the same daytime, and lower case letters indicate the effects of the daytime under the same treatment. (Control: treatment with sterile distilled water; Control+1: untreated leaves from the distal node from the control; flg22: treatment with 5 μM flagellin dissolved in sterile distilled water; flg22 + 1: untreated leaves from the distal node from the flg22-treated one).

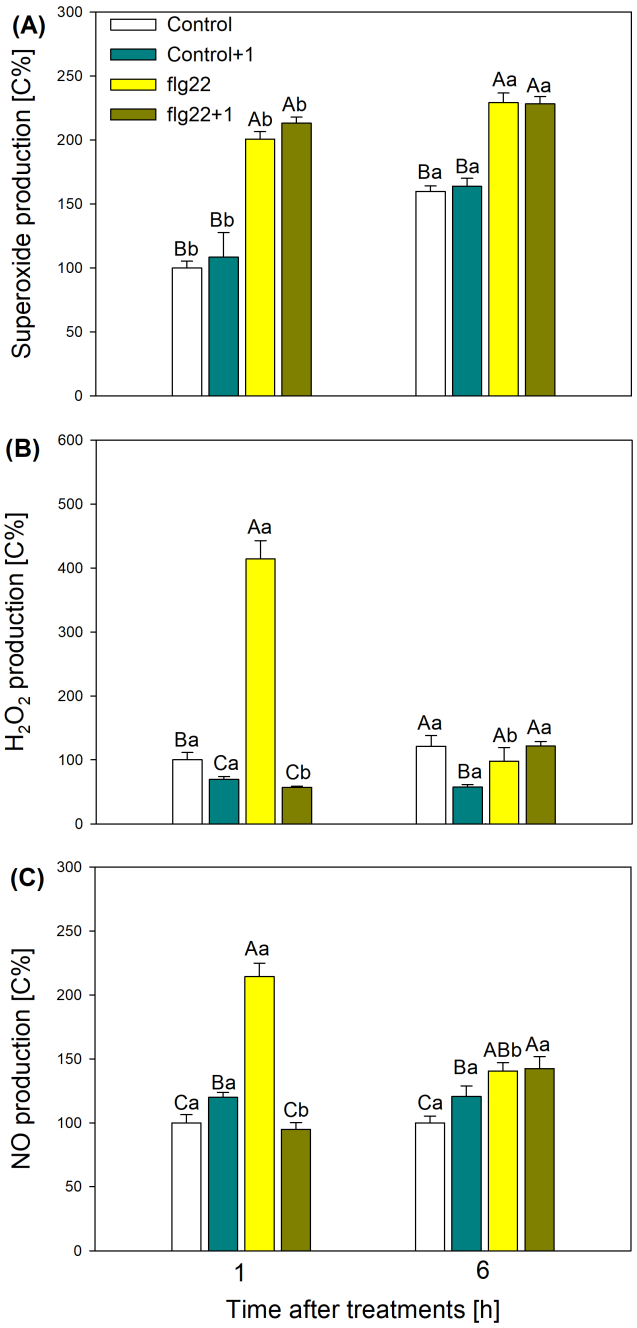

FIGURE 3 Time-dependent regulation of the metabolism of reactive oxygen species in the stomata. Changes in the superoxide (A), hydrogen peroxide (B) and nitric oxide (C) production were examined in the abaxial epidermal strips of intact tomato plants treated foliar with 5 μM flagellin (flg22) at 8:00 a.m. Measurements were carried out one and six hours later after treatments (at 9:00 a.m. and 14:00 p.m.). Means ± SE, n = 3. Means were analysed by two-way ANOVA, significant differences among the data were analysed by Duncan's test. Mean values significantly different at $p < 0.05$ were signed with different letters, upper case letters indicate the effects of the treatment at the same daytime, and lower case letters indicate the effects of the daytime under the same treatment. (Control: treatment with sterile distilled water; Control+1: untreated leaves from the distal node from the control; flg22: treatment with 5 μM flagellin dissolved in sterile distilled water; flg22 + 1: untreated leaves from the distal node from the flg22-treated one).

maintained for 6 hours in Arabidopsis (Devireddy et al., 2020; Fichman and Mittler, 2021). At the same time, the degree and signalling of stomatal closure may be highly dependent on the circadian rhythm (Webb, 2003; Hotta et al., 2007) as well as on the photosynthetic activity of guard cells (Lemonnier and Lawson, 2024). It is known that in addition to ions such as potassium, the production of osmotically active sugars by active photosynthesis in guard cells and in cooperation with mesophyll cells contributes to the control of guard cell turgor pressure and thus influences stomatal aperture sizes differently in the morning and afternoon (Lawson and Matthews, 2020). In this respect, stomatal closure was significant 6 h after the flg22 treatments, but not as significant as in the morning. In addition, the pore size of the stomata of the control plants was also reduced in the afternoon (Figure 1). Other results, such as the differences in ROS and NO production, JA levels and signalling in the afternoon compared to the morning suggest that flg22-induced defense responses at organ- and cell level are time-dependent and may be under diurnal regulation, especially in the case of guard cells.

Since flg22-induced production of signalling compounds such as ROS (Li and Kim, 2022) and NO (Sami et al., 2018), as well as the synthesis of key defense-related phytohormones such as JA (Wasternack and Hause, 2019) which are associated with the chloroplasts, the effects of flg22 on the photosynthetic activity of mesophyll cells as well as stomata were investigated. It was also previously observed that the effects of flg22 are highly dependent on light (Sano et al., 2014). Göhre et al., (2012) investigated the short- and long-term effects of flg22 on the photosynthetic activity in Arabidopsis seedlings grown in liquid medium and they found that flg22 induced the decrease of ΦPSII and the increase of NPQ after seven days (Göhre et al., 2012). At the same time, in our previous work investigating the diurnal effects of flg22 treatments and comparing the effects of flg22 in the light and dark periods on guard and mesophyll cells (Czékus et al., 2022), flg22 exposure caused a decrease in ΦPSII and a slight increase in NPQ in the stomata of the elicitor-treated leaves in the afternoon light period, while flg22 did not significantly affect mesophyll photosynthetic activity independently of the day/night period (Czékus et al., 2022). Based on recent experiments, guard cell photosynthesis was more sensitive to flg22 as compared to the mesophyll and flg22 decreased ΦPSII (Figure 2C) and qP (Figure 2E), while in parallel increased NPQ (Figure 2G) in stomata. Since stomata are located in the epidermal layer and were first exposed to flg22, the effects of flg22 on the photosynthetic activity of guard cells may be crucial in determining long-lasting stomatal closure as a part of plant defense responses (Czékus et al., 2022). These effects of flg22 on stomatal photosynthetic activity may depend on rapid ROS production mediated by NADPH oxidase (Ranf et al., 2011; Thor and Peiter, 2014) and later on ROS and NO production by chloroplasts in a self-amplifying loop that contributes to long-lasting stomatal closure and activation of defense signalling (Kangasjärvi et al., 2012), perhaps in stomata.

It was shown that ROS production in the stomata of the flg22-treated leaves was significantly higher as compared to the control after 1 hour, confirming that flg22 induced rapid ROS production (Robatzek et al., 2007; Lyons et al., 2013; Shi et al., 2013) which can

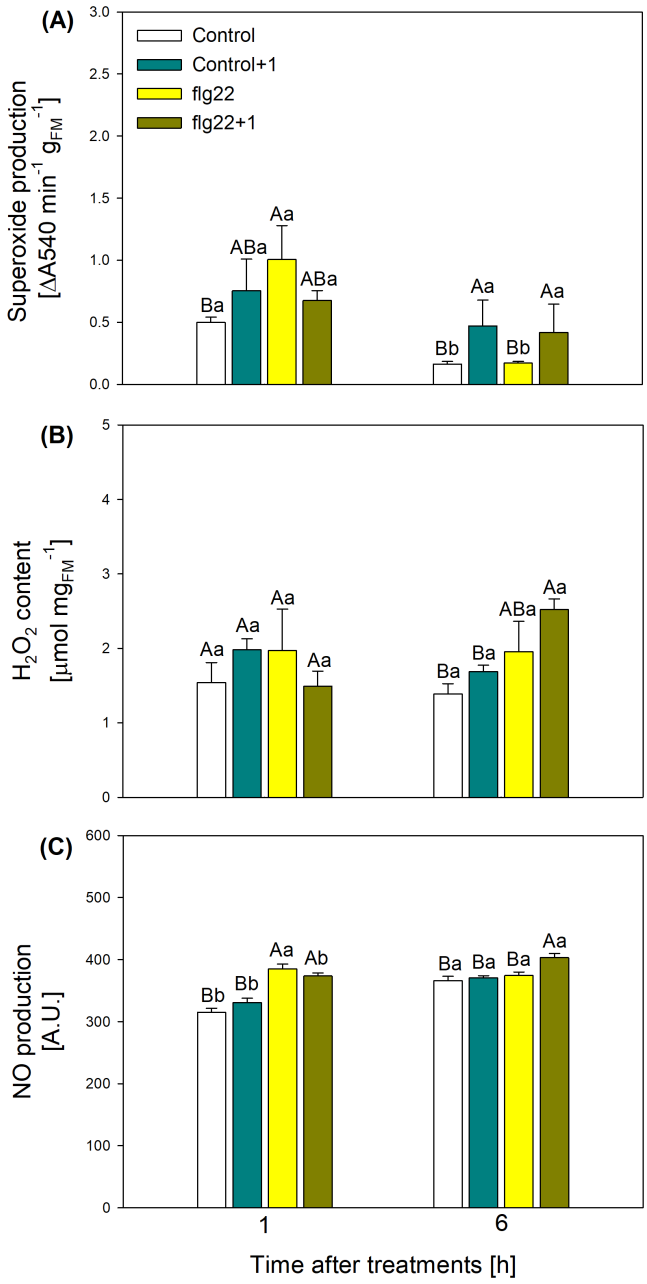

FIGURE 4 Time-dependent regulation of the metabolism of reactive oxygen species in leaves of intact tomato plants. Changes in the superoxide production (A), hydrogen peroxide content (B), and nitric oxide production (C) were examined in leaves of intact tomato plants treated foliar with 5 µM flagellin (flg22) at 8:00 a.m. Measurements were carried out one and six hours later after treatments (at 9:00 a.m. and 14:00 p.m.). Means ± SE, n = 3. Mean values significantly different at $p < 0.05$ were signed with different letters, upper case letters indicate the effects of the treatment at the same daytime, and lower case letters indicate the effects of the daytime under the same treatment. (Control: treatment with sterile distilled water; Control+1: untreated leaves from the distal node from the control; flg22: treatment with 5 µM flagellin dissolved in sterile distilled water; flg22 + 1: untreated leaves from the distal node from the flg22-treated one).

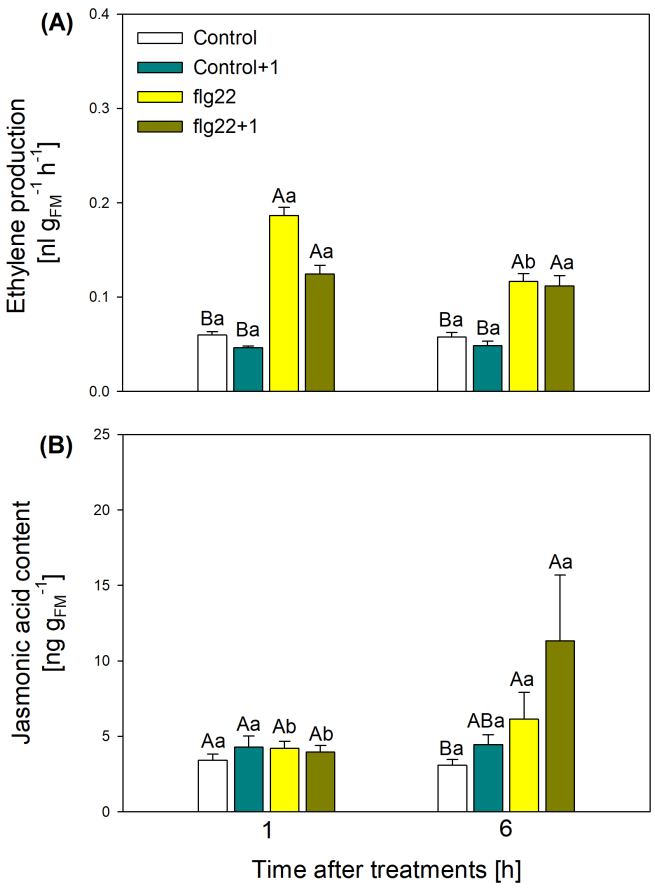

FIGURE 5 Time-dependent regulation of the metabolism of defense-related hormones. Changes in the ethylene (A) and jasmonic acid (B) contents were examined in leaves of intact tomato plants treated foliar with 5 µM flagellin (flg22) at 8:00 a.m. Measurements were carried out one and six hours later after treatments (at 9:00 a.m. and 14:00 p.m.). Means ± SE, n = 3. Mean values significantly different at $p < 0.05$ were signed with different letters, upper case letters indicate the effects of the treatment at the same daytime, and lower case letters indicate the effects of the daytime under the same treatment. (Control: treatment with sterile distilled water; Control+1: untreated leaves from the distal node from the control; flg22: treatment with 5 µM flagellin dissolved in sterile distilled water; flg22 + 1: untreated leaves from the distal node from the flg22-treated one).

contribute to stomatal closure (Sierla et al., 2016; Toum et al., 2016) and can origin from the chloroplast of stomata (Poór and Tari, 2012). NO also takes part in the regulation of stomatal closure upon pathogen infection (Mur et al., 2006; Zhang et al., 2008). Earlier other researchers also found that NO production increased only several hours later of the flg22 treatments in maize leaf disks (Zhang et al., 2017). At the same time, based on our former results (Czékus et al., 2021b), flg22 induced local and systemic NO production in 1 h in leaves of tomato plants which were dependent on the day/night period. Interestingly, based on our experiments, depending on the time point as well as on the type of tissue, ROS production leading to

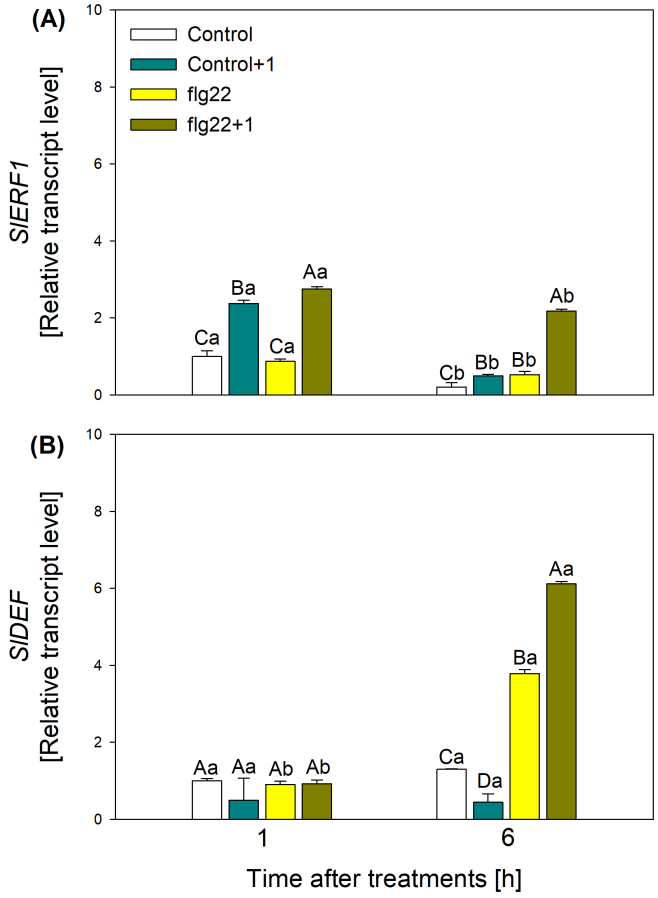

FIGURE 6 Time-dependent regulation of defense-related gene expression. Changes in the expression of *SlERF1* (A) and *SlDEF* (B) were examined in leaves of intact tomato plants treated foliar with 5 μM flagellin (flg22) at 8:00 a.m. Measurements were carried out one and six hours later after treatments (at 9:00 a.m. and 14:00 p.m.). Means ± SE, n = 3. Means were analysed by two-way ANOVA, significant differences among the data were analysed by Duncan's test. Mean values significantly different at $p < 0.05$ were signed with different letters, upper case letters indicate the effects of the treatment at the same daytime, and lower case letters indicate the effects of the daytime under the same treatment. (Control: treatment with sterile distilled water; Control+1: untreated leaves from the distal node from the control; flg22: treatment with 5 μM flagellin dissolved in sterile distilled water; flg22 + 1: untreated leaves from the distal node from the flg22-treated one).

stomatal closure seems to be limited directly to guard cells or to the entire leaf. Early stomatal closure 1 h following flg22 treatments could be triggered by both stomatal ROS, superoxide (Figure 3A), H_2O_2 (Figure 3B) and NO (Figure 3C) production, as well as elevated superoxide (Figure 4A) and NO (Figure 4C) accumulation in the entire leaf tissue which were significantly higher as compared to ROS/NO levels in the control tissues. However, systemic stomatal closure in the flg22 + 1 leaves could be a consequence of significantly higher superoxide production in stomata (Figure 3A) and NO production in the whole leaf (Figure 4C) at the first hour after flg22 treatment. It is well known that NO can act together with ROS influencing each other's synthesis and defense responses of plants contributing to phytohormones (Saleem et al., 2021; Vlot et al., 2021). Moreover NO plays also a role in the long-term systemic responses of plants (Agurla et al., 2020; Jahnová et al., 2020) such as regulating callose formation in the early phase of the infection (Xiao et al., 2018). Interestingly, the superoxide production increased only in the guard cells of systemic, flg22 + 1 leaves 6 h after the flg22 treatment (Figure 3A), while NO production was significantly higher at this time point both in the stomata of flg22-treated and systemic leaves of tomato (Figure 3C). Besides the stomatal ROS and NO production, flg22 increased H_2O_2 (Figure 4B) and NO levels (Figure 4C) after 6 h in the systemic leaves but neither ROS nor NO levels changed significantly in the flg22-treated leaves after 6 h. These results indicate that while NO production in the guard cells can result in local stomatal closure 6 h after flg22 treatments, in the systemic flg22 + 1 leaves, it can be originated by both increased superoxide and NO production in the guard cells as well as in the entire leaves. While in the leaves, superoxide production did not change significantly after 6 h, the level of H_2O_2 elevated systemically after 6 h of flg22 treatment (Figure 4B) which was not detected in the stomata (Figure 3B). It can be explained by the increased activity of superoxide dismutase catalyzing the conversion of superoxide into H_2O_2 and molecular oxygen which is regulated by phytohormones such as JA or ET under long-term defense responses of plants (Singh and Shah, 2014; Takács et al., 2018). Moreover, both defense-related phytohormones regulate ROS and NO production, as well as stomatal closure in Arabidopsis (Islam et al., 2009; Wang et al., 2020).

In addition to ROS and NO, the production of ET was rapidly induced by flg22 treatments, both locally and systemically, and was still detectable after 6 hours (Figure 5A). Furthermore, the expression of the ET marker gene *SlERF1* was induced in the systemic leaves after 1 h and in both the flg22-treated and systemic leaves after 6 h, but the most significant changes were observable in the systemic leaves after 6 h (Figure 6A). It is known that ET plays a crucial role in the early defense responses of plants after flg22 treatments, whereas late defense responses may be under the regulation of other phytohormones such as SA or JA (Mur et al., 2008; Mersmann et al., 2010; Wang et al., 2018). Recently, it was also shown that flg22 induces not only local but also systemic ET emission in leaves of intact tomato plants, which plays a crucial role in the regulation of ROS production in systemic leaves (Czékus et al., 2023). Volatile phytohormones such as ET, methyl jasmonic acid (MeJA) or methyl salicylic acid (MeSA) are capable of rapid transport due to their state, which is essential for both local and systemic defense (Gao et al., 2021). Our results further confirmed that ET can regulate both local and systemic ROS production, which in turn can determine stomatal movements 1 h as well as 6 h after the flg22 treatments.

After the initial peak of ET release induced by phytopathogen infection or flg22 elicitor treatments (Mur et al., 2008; Mersmann et al., 2010), late defense responses can be regulated by other phytohormones such as JA or SA (Wang et al., 2018). It is well known that ET can not only induce the production of ROS/NO and the expression of various defense response genes such as *PR-3-type basic chitinase*

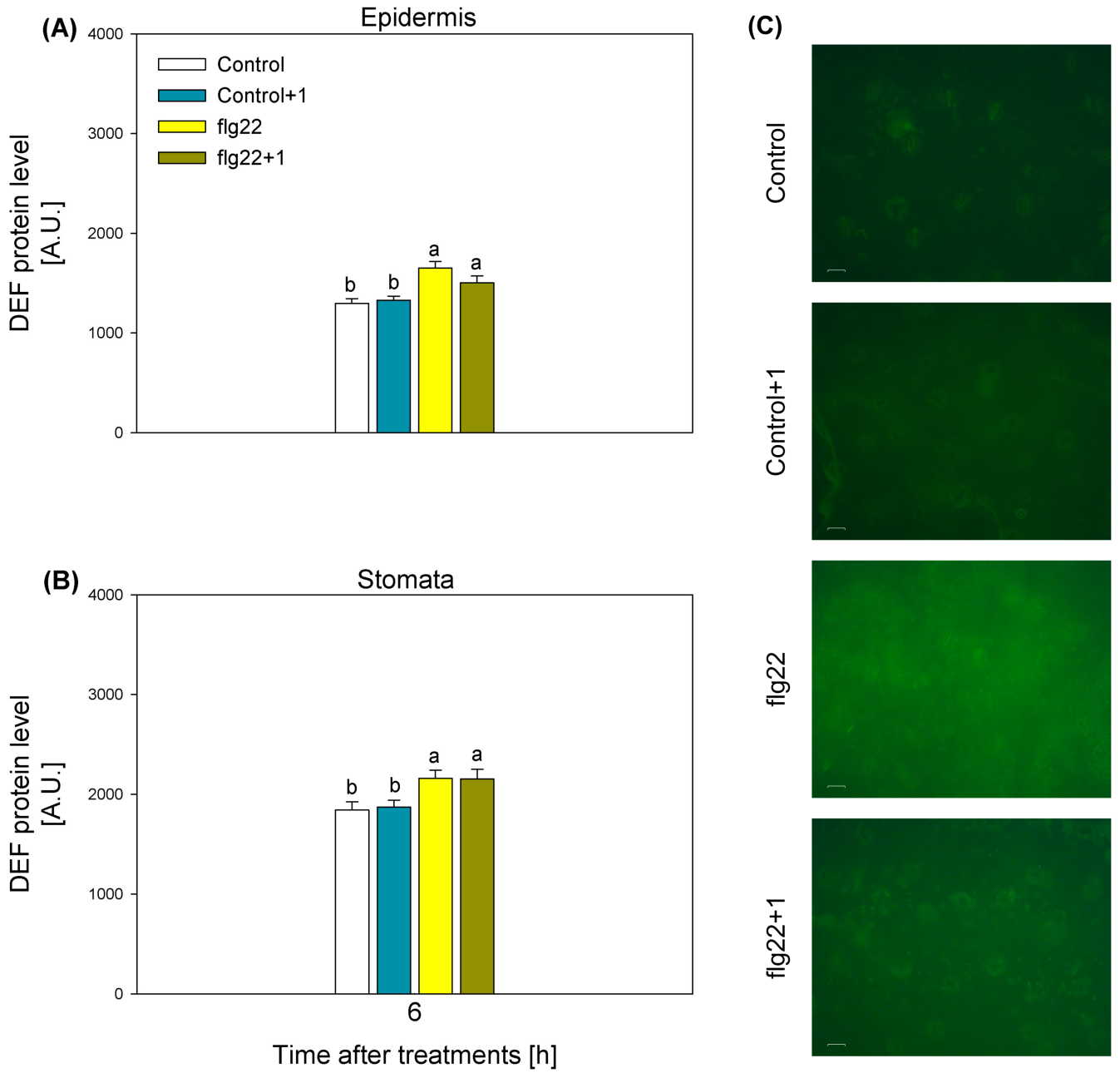

FIGURE 7 Changes in the defensin (DEF) protein levels. Protein accumulation was examined in the epidermal cells (A) and stomata (B) from the leaves of intact tomato plants treated foliar with 5 μM flagellin (flg22) at 8:00 a.m. (C: representative images). Measurements were carried out six hours later after treatments (at 14:00 p.m.). Means ± SE, n = 3. Means were analysed by one-way ANOVA, significant differences among the data were analysed by Duncan's test. Mean values significantly different at $p < 0.05$ were signed with different letters (Control: treatment with sterile distilled water; Control+1: untreated leaves from the distal node from the control; flg22: treatment with 5 μM flagellin dissolved in sterile distilled water; flg22 + 1: untreated leaves from the distal node from the flg22-treated one).

and *PR-4-type hevein-like protein* but also the induction of JA-related *PDF1.2 defensin* in Arabidopsis (van Loon et al., 2006). At the same time, ET may act synergistically with JA to mediate defense signalling, as has been previously shown in many cases of pathogen infection (Hase et al., 2003; Block et al., 2005; Mur et al., 2008). Our results also showed that flg22 application in the morning increased JA levels in leaves 6 h later in the afternoon in both flg22-treated and systemic leaves (Figure 5B). Moreover, the increased expression of the JA-regulated *SlDEF* also showed similar trends (Figure 6B), suggesting the key role of JA in the regulation of late defense responses upon flg22 exposure in tomato. Other researchers also measured higher JA levels after 8 h of flg22 exposure in Arabidopsis (Gravino et al., 2015), but higher SA levels were also observed in the late phase, e.g. after 24 h, suggesting that much later responses to flg22 are mostly mediated by SA (Denoux et al., 2008). Furthermore, basal levels of SA and JA, and thus plant immune responses, are regulated by the circadian

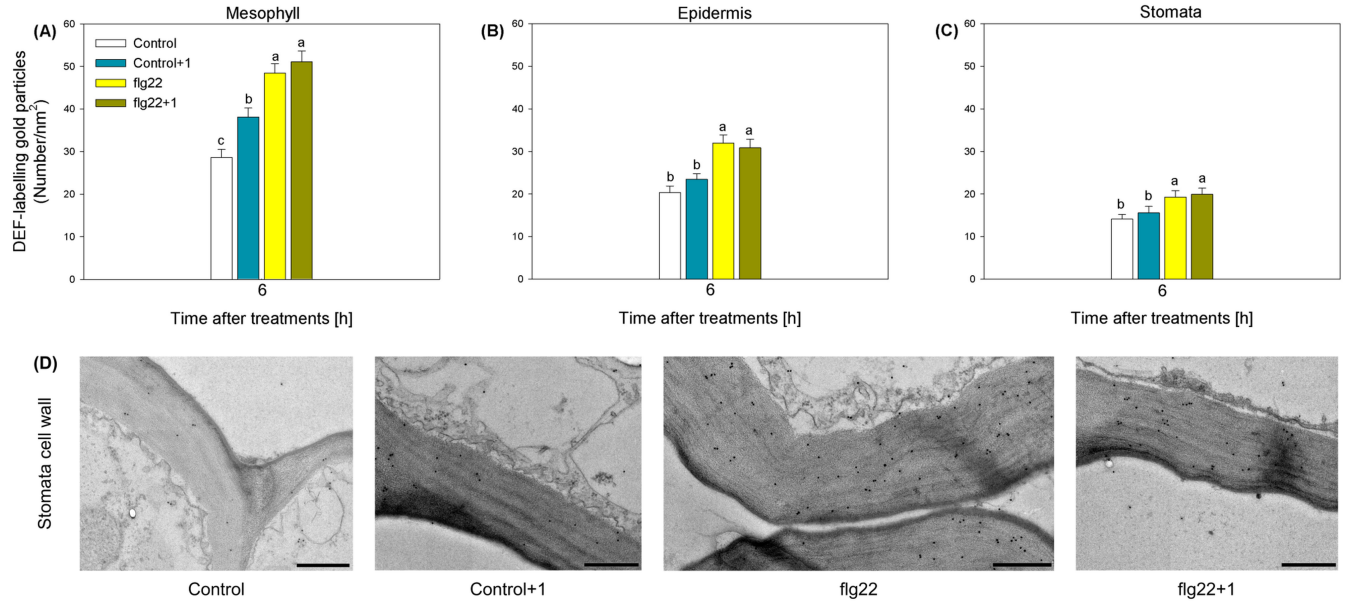

FIGURE 8 Changes in the defensin (DEF) protein accumulation. DEF protein levels were examined in the cell walls of mesophyll cells (A), epidermal cells (B) and stomata (C) from the leaves of intact tomato plants treated foliar with 5 μM flagellin (flg22) at 8:00 a.m. using immunogold labelling (D: representative images from stomata cell wall). Measurements were carried out six hours later after treatments (at 14:00 p.m.). Means ± SE, n = 3. Means were analysed by one-way ANOVA, significant differences among the data were analysed by Duncan's test. Mean values significantly different at $p < 0.05$ were signed with different letters (Control: treatment with sterile distilled water; Control+1: untreated leaves from the distal node from the control; flg22: treatment with 5 μM flagellin dissolved in sterile distilled water; flg22 + 1: untreated leaves from the distal node from the flg22-treated one).

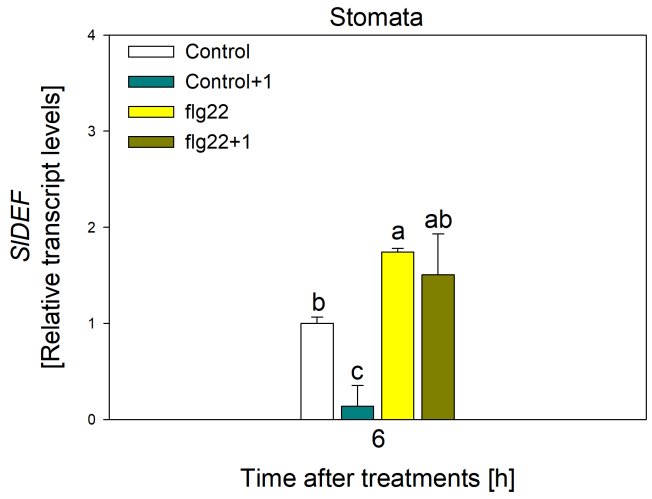

FIGURE 9 Changes in the expression of tomato *defensin* (*SlDEF*) in the stomata. Gene expression was examined in the leaves of intact tomato plants treated foliar with 5 μM flagellin (flg22) at 8:00 a.m. using single cell qRT-PCR. Measurements were carried out six hours later after treatments (at 14:00 p.m.). Means ± SE, n = 3. Means were analysed by one-way ANOVA, significant differences among the data were analysed by Duncan's test. Mean values significantly different at $p < 0.05$ were signed with different letters (Control: treatment with sterile distilled water; Control+1: untreated leaves from the distal node from the control; flg22: treatment with 5 μM flagellin dissolved in sterile distilled water; flg22 + 1: untreated leaves from the distal node from the flg22-treated one).

clock during the day, with JA accumulation peaking in the middle of the light period, whereas SA levels are the highest around the middle of the dark period at night (Zheng et al., 2015; Lu et al., 2017). Therefore, our results confirmed for the first time that flg22-induced defense signalling is regulated in a different way in the first minutes and hours, suggesting that the circadian regulation of flg22-induced defense responses is mediated by plant hormones, in which ET can be pivotal in the early phase (induced within 1 h), while both ET and JA are crucial in the late phase (induced after 6 h) of defense signalling. Moreover, JA can have a crucial role in this process not only locally but also systemically. This hypothesis was investigated further by analysing the expression of genes involved in defense hormone responses.

The significant ET/JA accumulation and *SlDEF* expression after 6 h of flg22 treatments in the local and systemic leaves suggest that plants are actively defended systemically by synthesising plant defensins before the dark period. Defensins are antimicrobial peptides that can interact with membrane lipids and interfere with their biological role (Sher Khan et al., 2019). Previously, significant *defensin* (*PDF1.1*) expression was found locally and systemically in the leaves of *Alternaria brassicicola*-infected Arabidopsis plants, which was also dependent on ET and JA, but independent of SA (Penninckx et al., 1996, 1998). Here, we observed not only the increased gene expression of *SlDEF* (Figure 6B) but also the accumulation of defensins in the epidermis (Figure 7A) as well as in the stomata (Figure 7B) of elicitor-treated leaves after 6 h of flg22 exposure. These results firstly confirmed that

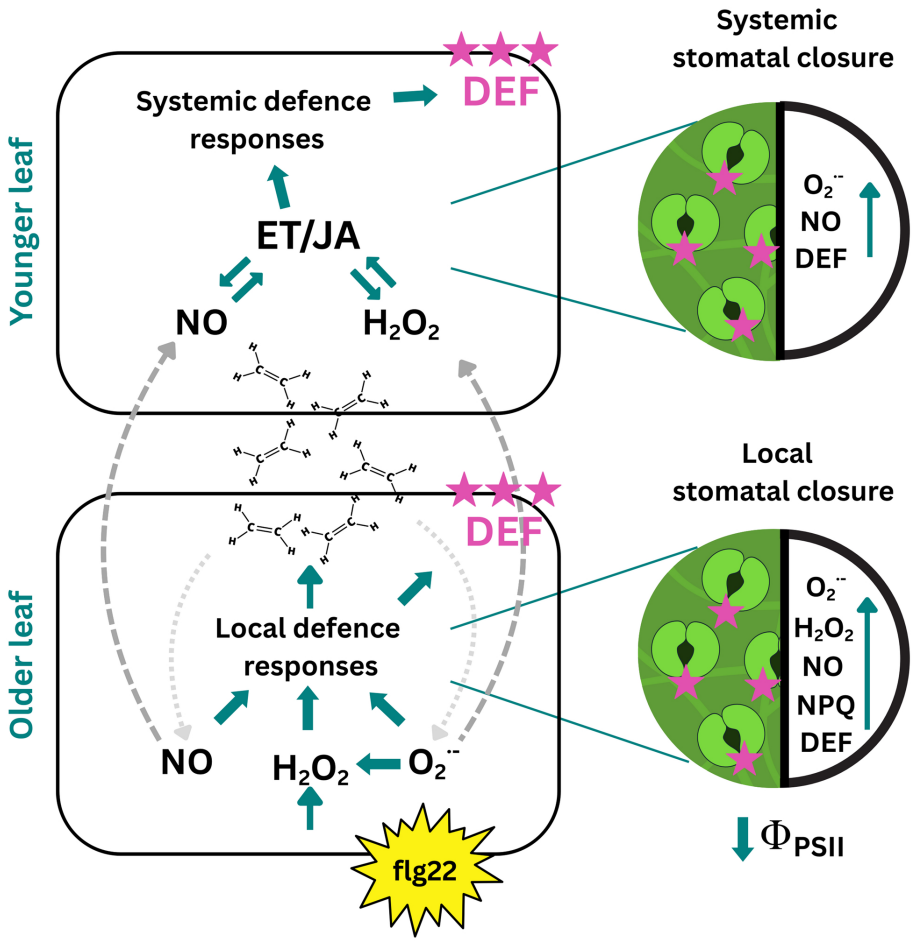

FIGURE 10 Schematic model of the induction of defensin (DEF) accumulation during flg22-induced local and systemic defence responses in leaves and stomata of tomato plants. Flg22 induces rapid local reactive oxygen species (ROS) and nitric oxide (NO) accumulation and ethylene (ET) emission, which contribute to the activation of local leaf defence responses, including stomatal closure. ROS and NO accumulation and reduced photosynthetic activity (ΦPSII) in guard cells contribute to this process. Local ROS/NO production and ET emission after flg22 treatment trigger not only local but also systemic defence responses, inducing jasmonic acid (JA) accumulation and stomatal closure. As part of the local and systemic defence responses of plants, the antimicrobial DEFs are accumulated in the cell wall of the mesophyll, epidermis and stomata.

flg22 treatments induce effective defense responses in plants by accumulating defensins both locally and systemically in elicitor-treated plants. Furthermore, these results suggested an active defense of cells such as epidermal or guard cells, which are part of the overall plant defense at the organ and individual level. In addition, immunogold labelling results clearly showed that defensins accumulated in the cell walls of the investigated cell types after flg22 treatments (Figure 8), with the highest levels in the cell wall of the mesophyll palisade parenchyma (Figure 8A) and the lowest levels in the cell walls of guard cells (Figure 8C). At the same time, the significant accumulation of defensins in the cell wall of guard cells (especially at the area where the two guard cells meet and close), where various phytopathogens can enter into the mesophyll (Melotto et al., 2006), showed for the first time that plants defend themselves by accumulating antimicrobial defensins already at the pore where phytopathogens can penetrate (Figure 8D). At the same time, defensins as water-soluble molecules presumably can be transported to the epidermis and stomata e.g. via water vapour diffusion in the cell wall. However, it was an important question whether guard cells themselves could synthesize defensin (Guzmán-Delgado et al., 2021). Based on the results of our single cell qRT-PCR, it can be concluded that the guard cells of flg22-treated and flg22 + 1 leaves were able to activate their defense and protection mechanisms via the increased expression of *SlDEF* (Figure 9). Thus, it can be concluded that cells located outside the mesophyll are not only involved in the first line of plant defense, but also participate in the active defense of the plants as a function of time and also defend themselves by producing and accumulating antimicrobial DEF after sensing the presence of the bacterial elicitor flg22 on the leaf surface.

5 | CONCLUSIONS

The present experiments demonstrated that flg22 induced rapid and long-lasting local and systemic defense responses and stomatal closure in the leaves of tomato plants (Figure 10). The flg22 treatments had a more significant effect on the photosynthetic activity of guard cells than that of mesophyll cells. However, this was only detectable in the first hour, based on decreased ΦPSII and qP and the increased NPQ. Consequently, these alterations can determine both the immediate and long-term stomatal closure of plants, which was also evident in the local and systemic leaves of intact plants. The impact of flg22 on photosynthetic activity may be contingent on the accumulation of ROS and NO, which, in addition to stomatal closure, can elicit defense signaling in stomata and the entire plant. However, the dynamics of this accumulation varied between cell types and across the diurnal cycle in both local and systemic leaves and stomata. The prolonged, local stomatal closure was found to be associated with superoxide/

NO production in the guard cells, while the accumulation of these substances in the entire leaf appeared to be implicated in the induction of swift, systemic stomatal closure. Plant defense hormones have been demonstrated to play a pivotal role in the regulation of ROS/NO levels, including ET and JA. Although the flg22-triggered ET production after 1 and 6 h could contribute to rapid and long-lasting local and systemic stomatal closure, the accumulation of JA increased only after 6 h, mainly in the local tissues. This indicates that the two hormones can mediate late defense signaling. This finding was further corroborated by the increased expression of *SlDEF* at this time point, as well as the increased accumulation of DEF proteins in the mesophyll, epidermis and guard cells of local and systemic leaves. In this study, defensin protein accumulation was first demonstrated after flg22 treatment in the cell walls of these cell types. Furthermore, single-cell qRT-PCR analyses confirmed that guard cells are capable of synthesizing defensin in both local and systemic leaves of intact plants. Therefore, it can be concluded that guard cells, in addition to representing the first line of plant defense through the regulation of stomatal pore size, may also be capable of defending themselves and the plant by producing and accumulating antimicrobial defensins where phytopathogens can penetrate inside the plants. Consequently, these findings have broader ecological and agricultural implications, as flg22-induced stomatal closure and defense responses could enhance plant resistance against microbial pathogens, reducing the need for chemical pesticides. Thus, understanding the molecular background of plant defense responses triggered by flg22 can provide new perspectives for breeding or biotechnological approaches to improve crop resilience under pathogen challenges, contributing to the development of new, innovative agricultural tools for sustainable crop production.

AUTHOR CONTRIBUTIONS

P.P. conceptualized the idea for the experiments. Z.C., A.K., A.M., B.P., Á.M., A.Ö., Gy.V., L.G., R.P., L.T., K.Á.K., N.F., N.B., M.B., G.Sz., Á.K.H. and P.P. carried out the experiments. Z.C. and P.P. wrote the original draft of the manuscript. Z.C., A.Ö., L.G., N.F., N.B., G.Sz. and P.P. reviewed and edited the manuscript. All the authors have read and approved the final version of the manuscript.

ACKNOWLEDGMENTS

We thank Bécs Attiláné for her excellent technical assistance.

FUNDING INFORMATION

This work was supported by grants from the National Research, Development and Innovation Office of Hungary - NKFIH (Grant No. NKFIH FK 124871, 138867 and PD146980), the ÚNKP-23-4 and ÚNKP-22-5 New National Excellence Program of the Ministry for Innovation and Technology, the Scientia Amabilis Foundation of the Hungarian Society for Plant Biology and the University of Szeged Open Access Fund (7050).

CONFLICT OF INTEREST STATEMENT

The authors declare that they have no competing interests.

DATA AVAILABILITY STATEMENT

The data that support the findings of this study are available from the corresponding author upon reasonable request.

ORCID

Zalán Czékus https://orcid.org/0000-0001-5862-1350
András Kukri https://orcid.org/0000-0002-6992-6018
Attila Ördög https://orcid.org/0000-0002-1867-8237
Nikolett Bódi https://orcid.org/0000-0002-9774-1387
Mária Bagyánszki https://orcid.org/0000-0003-3533-9461
Kamirán Áron Hamow https://orcid.org/0000-0002-7089-1078
Péter Poór https://orcid.org/0000-0002-4539-6358

REFERENCES

Agurla, S., Sunitha, V., & Raghavendra, A. S. (2020). Methyl salicylate is the most effective natural salicylic acid ester to close stomata while raising reactive oxygen species and nitric oxide in Arabidopsis guard cells. *Plant Physiology and Biochemistry*, 157, 276–283.

Ashraf, U., Hussain, S., Naveed Shahid, M., Anjum, S. A., Kondo, M., Mo, Z., & Tang, X. (2022). Alternate wetting and drying modulated physio-biochemical attributes, grain yield, quality, and aroma volatile in fragrant rice. *Physiologia Plantarum*, 174(6), e13833.

Aslam, S. N., Erbs, G., Morrissey, K. L., Newman, M. A., Chinchilla, D., Boller, T., … & Cooper, R. M. (2009). Microbe-associated molecular pattern (MAMP) signatures, synergy, size and charge: influences on perception or mobility and host defence responses. *Molecular Plant Pathology*, 10(3), 375–387.

Block, A., Schmelz, E., O'Donnell, P. J., Jones, J. B., & Klee, H. J. (2005). Systemic acquired tolerance to virulent bacterial pathogens in tomato. *Plant Physiology*, 138(3), 1481–1490.

Brasko, C., Smith, K., Molnar, C., Farago, N., Hegedus, L., Balind, A., … & Horvath, P. (2018). Intelligent image-based in situ single-cell isolation. *Nature Communications*, 9(1), 226.

Bright, J., Desikan, R., Hancock, J. T., Weir, I. S., & Neill, S. J. (2006). ABA-induced NO generation and stomatal closure in Arabidopsis are dependent on H_2O_2 synthesis. *The Plant Journal*, 45(1), 113–122.

Czékus, Z., Iqbal, N., Pollák, B., Martics, A., Ördög, A., & Poór, P. (2021a). Role of ethylene and light in chitosan-induced local and systemic defence responses of tomato plants. *Journal of Plant Physiology*, 263, 153461.

Czékus, Z., Kukri, A., Hamow, K. Á., Szalai, G., Tari, I., Ördög, A., & Poór, P. (2021b). Activation of local and systemic defence responses by Flg22 is dependent on daytime and ethylene in intact tomato plants. *International Journal of Molecular Sciences*, 22(15), 8354.

Czékus, Z., Koprivanacz, P., Kukri, A., Iqbal, N., Ördög, A., & Poór, P. (2022). The role of photosynthetic activity in the regulation of flg22-induced local and systemic defence reaction in tomato. *Photosynthetica*, 60(2), 1–12.

Czékus, Z., Martics, A., Pollák, B., Kukri, A., Tari, I., Ördög, A., & Poór, P. (2023). The local and systemic accumulation of ethylene determines the rapid defence responses induced by flg22 in tomato (*Solanum lycopersicum* L.). *Journal of Plant Physiology*, 287, 154041.

DeFalco, T. A., & Zipfel, C. (2021). Molecular mechanisms of early plant pattern-triggered immune signaling. *Molecular Cell*, 81(17), 3449–3467.

Deger G., A., Scherzer, S., Nuhkat, M., Kedzierska, J., Kollist, H., Brosché, M., … & Roelfsema, M. R. G. (2015). Guard cell SLAC 1-type anion channels mediate flagellin-induced stomatal closure. *New Phytologist*, 208(1), 162–173.

Denoux, C., Galletti, R., Mammarella, N., Gopalan, S., Werck, D., De Lorenzo, G., … & Dewdney, J. (2008). Activation of defense response pathways by OGs and Flg22 elicitors in Arabidopsis seedlings. *Molecular Plant*, 1(3), 423–445.

Devireddy, A. R., Liscum, E., & Mittler, R. (2020). Phytochrome B is required for systemic stomatal responses and reactive oxygen species signaling during light stress. *Plant Physiology*, 184(3), 1563–1572.

Driesen, E., Van den Ende, W., De Proft, M., & Saeys, W. (2020). Influence of environmental factors light, CO_2, temperature, and relative humidity on stomatal opening and development: A review. *Agronomy*, 10(12), 1975.

Duxbury, Z., Wu, C. H., & Ding, P. (2021). A comparative overview of the intracellular guardians of plants and animals: NLRs in innate immunity and beyond. *Annual Review of Plant Biology*, 72, 155–184.

Fichman, Y., & Mittler, R. (2021). Integration of electric, calcium, reactive oxygen species and hydraulic signals during rapid systemic signaling in plants. *The Plant Journal*, 107(1), 7–20.

Gallé, Á., Csiszár, J., Benyó, D., Laskay, G., Leviczky, T., Erdei, L., & Tari, I. (2013). Isohydric and anisohydric strategies of wheat genotypes under osmotic stress: biosynthesis and function of ABA in stress responses. *Journal of Plant Physiology*, 170(16), 1389–1399.

Gao, H., Guo, M., Song, J., Ma, Y., & Xu, Z. (2021). Signals in systemic acquired resistance of plants against microbial pathogens. *Molecular Biology Reports*, 48(4), 3747–3759.

Genty, B., Briantais, J. M., & Baker, N. R. (1989). The relationship between the quantum yield of photosynthetic electron transport and quenching of chlorophyll fluorescence. *Biochimica et Biophysica Acta (BBA)-General Subjects*, 990(1), 87–92.

Goh, C. H., Schreiber, U., & Hedrich, R. (1999). New approach of monitoring changes in chlorophyll a fluorescence of single guard cells and protoplasts in response to physiological stimuli. *Plant, Cell & Environment*, 22(9), 1057–1070.

Göhre, V., Jones, A. M., Sklenář, J., Robatzek, S., & Weber, A. P. (2012). Molecular crosstalk between PAMP-triggered immunity and photosynthesis. *Molecular Plant-Microbe Interactions*, 25(8), 1083–1092.

Gravino, M., Savatin, D. V., Macone, A., & De Lorenzo, G. (2015). Ethylene production in B otrytis cinerea-and oligogalacturonide-induced immunity requires calcium-dependent protein kinases. *The Plant Journal*, 84(6), 1073–1086.

Guzmán-Delgado, P., Laca, E., & Zwieniecki, M. A. (2021). Unravelling foliar water uptake pathways: The contribution of stomata and the cuticle. *Plant, Cell & Environment*, 44(6), 1728–1740.

Han, G. Z. (2019). Origin and evolution of the plant immune system. *New Phytologist*, 222(1), 70–83.

Hase, S., Van Pelt, J. A., Van Loon, L. C., & Pieterse, C. M. (2003). Colonization of Arabidopsis roots by *Pseudomonas fluorescens* primes the plant to produce higher levels of ethylene upon pathogen infection. *Physiological and Molecular Plant Pathology*, 62(4), 219–226.

Hillmer, R. A., Tsuda, K., Rallapalli, G., Asai, S., Truman, W., Papke, M. D., … & Katagiri, F. (2017). The highly buffered Arabidopsis immune signaling network conceals the functions of its components. *PLoS Genetics*, 13(5), e1006639.

Hotta, C. T., Gardner, M. J., Hubbard, K. E., Baek, S. J., Dalchau, N., Suhita, D., … & Webb, A. A. (2007). Modulation of environmental responses of plants by circadian clocks. *Plant, Cell & Environment*, 30(3), 333–349.

Islam, M. M., Tani, C., Watanabe-Sugimoto, M., Uraji, M., Jahan, M. S., Masuda, C., … & Murata, Y. (2009). Myrosinases, TGG1 and TGG2, redundantly function in ABA and MeJA signaling in Arabidopsis guard cells. *Plant and Cell Physiology*, 50(6), 1171–1175.

Jahnová, J., Činčalová, L., Sedlářová, M., Jedelská, T., Sekaninová, J., Mieslerová, B., … & Petřivalský, M. (2020). Differential modulation of S-nitrosoglutathione reductase and reactive nitrogen species in wild and cultivated tomato genotypes during development and powdery mildew infection. *Plant Physiology and Biochemistry*, 155, 297–310.

Johns, S., Hagihara, T., Toyota, M., & Gilroy, S. (2021). The fast and the furious: rapid long-range signaling in plants. *Plant Physiology*, 185(3), 694–706.

Kangasjärvi, Saijaliisa, Jenny Neukermans, Shengchun Li, Eva-Mari Aro, and Graham Noctor. Photosynthesis, photorespiration, and light signalling in defence responses. *Journal of Experimental Botany* 63, no. 4 (2012): 1619–1636.

Kolbert, Z., Molnár, Á., Kovács, K., Lipták-Lukácsik, S., Benkő, P., Szőllősi, R., … & Kónya, Z. (2023). Nitro-oxidative response to internalized multi-walled carbon nanotubes in *Brassica napus* and *Solanum lycopersicum*. *Ecotoxicology and Environmental Safety*, 267, 115633.

Kollist, H., Zandalinas, S. I., Sengupta, S., Nuhkat, M., Kangasjärvi, J., & Mittler, R. (2019). Rapid responses to abiotic stress: priming the landscape for the signal transduction network. *Trends in Plant Science*, 24(1), 25–37.

Korneli, C., Danisman, S., & Staiger, D. (2014). Differential control of preinvasive and post-invasive antibacterial defense by the Arabidopsis circadian clock. *Plant and Cell Physiology*, 55(9), 1613–1622.

Kramer, D. M., Johnson, G., Kiirats, O., & Edwards, G. E. (2004). New fluorescence parameters for the determination of QA redox state and excitation energy fluxes. *Photosynthesis Research*, 79, 209–218.

Kukri, A., Czékus, Z., Gallé, Á., Nagy, G., Zsindely, N., Bodai, L., … & Poór, P. (2024). Exploring the effects of red light night break on the defence mechanisms of tomato against fungal pathogen *Botrytis cinerea*. *Physiologia Plantarum*, 176(4), e14504.

Lawson, T., & Matthews, J. (2020). Guard cell metabolism and stomatal function. *Annual Review of Plant Biology*, 71, 273–302.

Lee, D., Lal, N. K., Lin, Z. J. D., Ma, S., Liu, J., Castro, B., … & Coaker, G. (2020). Regulation of reactive oxygen species during plant immunity through phosphorylation and ubiquitination of RBOHD. *Nature Communications*, 11(1), 1838.

Lemonnier, P., & Lawson, T. (2024). Calvin cycle and guard cell metabolism impact stomatal function. In *Seminars in Cell & Developmental Biology* (Vol. 155, pp. 59–70). Academic Press.

Li, M., & Kim, C. (2022). Chloroplast ROS and stress signaling. *Plant Communications*, 3(1).

Liu, H., Song, S., Zhang, H., Li, Y., Niu, L., Zhang, J., & Wang, W. (2022). Signaling transduction of ABA, ROS, and Ca^{2+} in plant stomatal closure in response to drought. *International Journal of Molecular Sciences*, 23(23), 14824.

Livak KJ, Schmittgen TD (2001) Analysis of relative gene expression data using real-time quantitative PCR and the $2^{-\ \Delta\Delta C}{}_{T}$ method. *Methods* 25:402–408

Lu, H., McClung, C. R., & Zhang, C. (2017). Tick tock: circadian regulation of plant innate immunity. *Annual Review of Phytopathology*, 55, 287–311.

Lyons, R., Iwase, A., Gänsewig, T., Sherstnev, A., Duc, C., Barton, G. J., … & Shirasu, K. (2013). The RNA-binding protein FPA regulates flg22-triggered defense responses and transcription factor activity by alternative polyadenylation. *Scientific Reports*, 3(1), 2866.

Matkowski, H., & Daszkowska-Golec, A. (2023). Update on stomata development and action under abiotic stress. *Frontiers in Plant Science*, 14, 1270180.

Meisrimler, C. N., Allan, C., Eccersall, S., & Morris, R. J. (2021). Interior design: how plant pathogens optimize their living conditions. *New Phytologist*, 229(5), 2514–2524.

Melotto, M., Underwood, W., Koczan, J., Nomura, K., & He, S. Y. (2006). Plant stomata function in innate immunity against bacterial invasion. *Cell*, 126(5), 969–980.

Melotto, M., Fochs, B., Jaramillo, Z., & Rodrigues, O. (2024). Fighting for Survival at the Stomatal Gate. *Annual Review of Plant Biology*, 75(1), 551–577.

Mersmann, S., Bourdais, G., Rietz, S., & Robatzek, S. (2010). Ethylene signaling regulates accumulation of the FLS2 receptor and is required for the oxidative burst contributing to plant immunity. *Plant Physiology*, 154(1), 391–400.

Millet, Y. A., Danna, C. H., Clay, N. K., Songnuan, W., Simon, M. D., Werck-Reichhart, D., & Ausubel, F. M. (2010). Innate immune responses activated in Arabidopsis roots by microbe-associated molecular patterns. *The Plant Cell*, 22(3), 973–990.

Mittler, R., Zandalinas, S. I., Fichman, Y., & Van Breusegem, F. (2022). Reactive oxygen species signalling in plant stress responses. *Nature Reviews Molecular Cell Biology*, 23(10), 663–679.

Montillet, J. L., Leonhardt, N., Mondy, S., Tranchimand, S., Rumeau, D., Boudsocq, M., … & Hirt, H. (2013). An abscisic acid-independent oxylipin pathway controls stomatal closure and immune defense in Arabidopsis. *PLoS Biology*, 11(3), e1001513.

Mur, L. A., Carver, T. L., & Prats, E. (2006). NO way to live; the various roles of nitric oxide in plant–pathogen interactions. *Journal of Experimental Botany*, 57(3), 489–505.

Mur, L. A., Laarhoven, L. J., Harren, F. J., Hall, M. A., & Smith, A. R. (2008). Nitric oxide interacts with salicylate to regulate biphasic ethylene production during the hypersensitive response. *Plant Physiology*, 148(3), 1537–1546.

Myers Jr, R. J., Fichman, Y., Zandalinas, S. I., & Mittler, R. (2023). Jasmonic acid and salicylic acid modulate systemic reactive oxygen species signaling during stress responses. *Plant Physiology*, 191(2), 862–873.

Myers, R. J., Peláez-Vico, M. Á., & Fichman, Y. (2024). *Functional analysis of reactive oxygen species-driven stress systemic signalling, interplay and acclimation*. *Plant*, Cell & Environment.

Nawaz, M., Sun, J., Shabbir, S., Khattak, W. A., Ren, G., Nie, X., … & Sonne, C. (2023). A review of plants strategies to resist biotic and abiotic environmental stressors. *Science of The Total Environment*, 165832.

Ngou, B. P. M., Ding, P., & Jones, J. D. (2022). Thirty years of resistance: Zig-zag through the plant immune system. *The Plant Cell*, 34(5), 1447–1478.

Pál, M., Ivanovska, B., Oláh, T., Tajti, J., Hamow, K. Á., Szalai, G., … & Janda, T. (2019). Role of polyamines in plant growth regulation of *Rht* wheat mutants. *Plant Physiology and Biochemistry*, 137, 189–202

Panchal, S., & Melotto, M. (2017). Stomate-based defense and environmental cues. *Plant Signaling & Behavior*, 12(9), e1362517.

Payá, C., Belda-Palazón, B., Vera-Sirera, F., Pérez-Pérez, J., Jordá, L., Rodrigo, I., … & Lisón, P. (2024). Signalling mechanisms and agricultural applications of (Z)-3-hexenyl butyrate-mediated stomatal closure. *Horticulture Research*, 11(1), uhad248.

Penninckx, I. A., Eggermont, K., Terras, F. R., Thomma, B. P., De Samblanx, G. W., Buchala, A., … & Broekaert, W. F. (1996). Pathogen-induced systemic activation of a plant defensin gene in Arabidopsis follows a salicylic acid-independent pathway. *The Plant Cell*, 8(12), 2309–2323.

Penninckx, I. A., Thomma, B. P., Buchala, A., Métraux, J. P., & Broekaert, W. F. (1998). Concomitant activation of jasmonate and ethylene response pathways is required for induction of a plant defensin gene in Arabidopsis. *The Plant Cell*, 10(12), 2103–2113.

Poór, P., & Tari, I. (2012). Regulation of stomatal movement and photosynthetic activity in guard cells of tomato abaxial epidermal peels by salicylic acid. *Functional Plant Biology*, 39(12), 1028–1037.

Poór, P., Kovács, J., Borbély, P., Takács, Z., Szepesi, Á., & Tari, I. (2015). Salt stress-induced production of reactive oxygen-and nitrogen species and cell death in the ethylene receptor mutant *Never ripe* and wild type tomato roots. *Plant Physiology and Biochemistry*, 97, 313–322.

Poór, P., Patyi, G., Takács, Z., Szekeres, A., Bódi, N., Bagyánszki, M., & Tari, I. (2019). Salicylic acid-induced ROS production by mitochondrial electron transport chain depends on the activity of mitochondrial hexokinases in tomato (*Solanum lycopersicum* L.). *Journal of Plant Research*, 132, 273–283.

Po-Wen, C., Singh, P., & Zimmerli, L. (2013). Priming of the Arabidopsis pattern-triggered immunity response upon infection by necrotrophic *Pectobacterium carotovorum* bacteria. *Molecular Plant Pathology*, 14(1), 58–70.

Ranf, S., Eschen-Lippold, L., Pecher, P., Lee, J., & Scheel, D. (2011). Interplay between calcium signalling and early signalling elements during defence responses to microbe-or damage-associated molecular patterns. *The Plant Journal*, 68(1), 100–113.

Robatzek, S., Bittel, P., Chinchilla, D., Köchner, P., Felix, G., Shiu, S. H., & Boller, T. (2007). Molecular identification and characterization of the tomato flagellin receptor LeFLS2, an orthologue of Arabidopsis FLS2 exhibiting characteristically different perception specificities. *Plant Molecular Biology*, 64, 539–547.

Rodrigues, O., Reshetnyak, G., Grondin, A., Saijo, Y., Leonhardt, N., Maurel, C., & Verdoucq, L. (2017). Aquaporins facilitate hydrogen peroxide entry into guard cells to mediate ABA-and pathogen-triggered stomatal closure. *Proceedings of the National Academy of Sciences*, 114(34), 9200–9205.

Roberts, R., Liu, A. E., Wan, L., Geiger, A. M., Hind, S. R., Rosli, H. G., & Martin, G. B. (2020). Molecular characterization of differences between the tomato immune receptors flagellin sensing 3 and flagellin sensing 2. *Plant Physiology*, 183(4), 1825–1837.

Saleem, M., Fariduddin, Q., & Castroverde, C. D. M. (2021). Salicylic acid: A key regulator of redox signalling and plant immunity. *Plant Physiology and Biochemistry*, 168, 381–397.

Sami, F., Faizan, M., Faraz, A., Siddiqui, H., Yusuf, M., & Hayat, S. (2018). Nitric oxide-mediated integrative alterations in plant metabolism to confer abiotic stress tolerance, NO crosstalk with phytohormones and NO-mediated post translational modifications in modulating diverse plant stress. *Nitric Oxide*, 73, 22–38.

Sanguankiattichai, N., Buscaill, P., & Preston, G. M. (2022). How bacteria overcome flagellin pattern recognition in plants. *Current Opinion in Plant Biology*, 67, 102224.

Sano, S., Aoyama, M., Nakai, K., Shimotani, K., Yamasaki, K., Sato, M. H., … & Shiina, T. (2014). Light-dependent expression of flg22-induced defense genes in Arabidopsis. *Frontiers in Plant Science*, 5, 104399.

Sher Khan, R., Iqbal, A., Malak, R., Shehryar, K., Attia, S., Ahmed, T., … & Mii, M. (2019). Plant defensins: types, mechanism of action and prospects of genetic engineering for enhanced disease resistance in plants. 3 *Biotech*, 9, 1–12.

Shi, H., Shen, Q., Qi, Y., Yan, H., Nie, H., Chen, Y., … & Tang, D. (2013). BR-SIGNALING KINASE1 physically associates with FLAGELLIN SENSING2 and regulates plant innate immunity in Arabidopsis. *The Plant Cell*, 25(3), 1143–1157.

Sierla, M., Waszczak, C., Vahisalu, T., & Kangasjärvi, J. (2016). Reactive oxygen species in the regulation of stomatal movements. *Plant Physiology*, 171(3), 1569–1580.

Singh, I., & Shah, K. (2014). Exogenous application of methyl jasmonate lowers the effect of cadmium-induced oxidative injury in rice seedlings. *Phytochemistry*, 108, 57–66.

Sobol, G., Majhi, B. B., Pasmanik-Chor, M., Zhang, N., Roberts, H. M., Martin, G. B., & Sessa, G. (2023). Tomato receptor-like cytoplasmic kinase Fir1 is involved in flagellin signaling and preinvasion immunity. *Plant Physiology*, 192(1), 565–581.

Takács, Z., Poór, P., Borbély, P., Czékus, Z., Szalai, G., & Tari, I. (2018). H2O2 homeostasis in wild-type and ethylene-insensitive *Never ripe* tomato in response to salicylic acid treatment in normal photoperiod and in prolonged darkness. *Plant Physiology and Biochemistry*, 126, 74–85.

Thor, K., & Peiter, E. (2014). Cytosolic calcium signals elicited by the pathogen-associated molecular pattern flg22 in stomatal guard cells are of an oscillatory nature. *New Phytologist*, 204(4), 873–881.

Toum, L., Torres, P. S., Gallego, S. M., Benavídes, M. P., Vojnov, A. A., & Gudesblat, G. E. (2016). Coronatine inhibits stomatal closure through guard cell-specific inhibition of NADPH oxidase-dependent ROS production. *Frontiers in Plant Science*, 7, 1851.

van Loon, L. C., Geraats, B. P., & Linthorst, H. J. (2006). Ethylene as a modulator of disease resistance in plants. *Trends in Plant Science*, 11(4), 184–191.

Vlot, A. C., Sales, J. H., Lenk, M., Bauer, K., Brambilla, A., Sommer, A., … & Nayem, S. (2021). Systemic propagation of immunity in plants. *New Phytologist*, 229(3), 1234–1250.

Wang, S., Zheng, Y., Gu, C., He, C., Yang, M., Zhang, X., … & Niu, D. (2018). Bacillus cereus AR156 activates defense responses to *Pseudomonas syringae* pv. *tomato* in Arabidopsis thaliana similarly to flg22. *Molecular Plant-Microbe Interactions*, 31(3), 311–322.

Wang, H. Q., Sun, L. P., Wang, L. X., Fang, X. W., Li, Z. Q., Zhang, F. F., … & He, J. M. (2020). Ethylene mediates salicylic-acid-induced stomatal closure by controlling reactive oxygen species and nitric oxide production in Arabidopsis. *Plant Science*, 294, 110464.

Wasternack, C., & Hause, B. (2019). The missing link in jasmonic acid biosynthesis. *Nature Plants*, 5(8), 776–777.

Webb, A. A. (2003). The physiology of circadian rhythms in plants. *New Phytologist*, 160(2), 281–303.

Wu, B., Qi, F., & Liang, Y. (2023). Fuels for ROS signaling in plant immunity. *Trends in Plant Science*, 28(10), 1124–1131.

Xiao, D., Duan, X., Zhang, M., Sun, T., Sun, X., Li, F., … & Wang, D. (2018). Changes in nitric oxide levels and their relationship with callose deposition during the interaction between soybean and Soybean mosaic virus. *Plant Biology*, 20(2), 318–326.

Zhang, X., Zhang, L., Dong, F., Gao, J., Galbraith, D. W., & Song, C. P. (2001). Hydrogen peroxide is involved in abscisic acid-induced stomatal closure in *Vicia faba*. *Plant Physiology*, 126(4), 1438–1448.

Zhang, W., He, S. Y., & Assmann, S. M. (2008). The plant innate immunity response in stomatal guard cells invokes G-protein-dependent ion channel regulation. *The Plant Journal*, 56(6), 984–996.

Zhang, X., Valdés-López, O., Arellano, C., Stacey, G., & Balint-Kurti, P. (2017). Genetic dissection of the maize (*Zea mays* L.) MAMP response. *Theoretical and Applied Genetics*, 130, 1155–1168.

Zheng, X. Y., Zhou, M., Yoo, H., Pruneda-Paz, J. L., Spivey, N. W., Kay, S. A., & Dong, X. (2015). Spatial and temporal regulation of biosynthesis of the plant immune signal salicylic acid. *Proceedings of the National Academy of Sciences*, 112(30), 9166–9173.

Zhou, J., Mu, Q., Wang, X., Zhang, J., Yu, H., Huang, T., … & Meng, X. (2022). Multilayered synergistic regulation of phytoalexin biosynthesis by ethylene, jasmonate, and MAPK signaling pathways in Arabidopsis. *The Plant Cell*, 34(8), 3066–3087.

Zou, M., Guo, M., Zhou, Z., Wang, B., Pan, Q., Li, J., … & Li, J. (2021). MPK3-and MPK6-mediated VLN3 phosphorylation regulates actin dynamics during stomatal immunity in Arabidopsis. *Nature Communications*, 12(1), 6474.

How to cite this article: Czékus, Z., Kukri, A., Martics, A., Pollák, B., Molnár, Á., Ördög, A. et al. (2025) Do guard cells have single or multiple defense mechanisms in response to flg22? *Physiologia Plantarum*, 177(3), e70249. Available from: https://doi.org/10.1111/ppl.70249